

International Doctorate Program in
Molecular Oncology and
Endocrinology
Doctorate School in Molecular
Medicine

XXII cycle - 2006–2009
Coordinator: Prof. Giancarlo Vecchio

**ROLE OF PAX8 TRANSCRIPTIONAL
FACTOR IN THE DIFFERENTIATED
THYROID**

PINA MAROTTA

University of Naples Federico II
Dipartimento di Biologia e Patologia Cellulare e Molecolare
“L. Califano”

Administrative Location

Dipartimento di Biologia e Patologia Cellulare e Molecolare “L. Califano”
Università degli Studi di Napoli Federico II

Partner Institutions

Italian Institutions

Università degli Studi di Napoli “Federico II”, Naples, Italy
Istituto di Endocrinologia ed Oncologia Sperimentale “G. Salvatore”, CNR,
Naples, Italy
Seconda Università di Napoli, Naples, Italy
Università del Sannio, Benevento, Italy
Università di Genova, Genoa, Italy
Università di Padova, Padua, Italy
Università degli Studi “Magna Graecia”, Catanzaro, Italy
Università degli Studi di Firenze, Florence, Italy
Università degli Studi di Bologna, Bologna, Italy
Università degli Studi del Molise, Campobasso, Italy
Università degli Studi di Torino, Turin, Italy
Università di Udine, Udine, Italy

Foreign Institutions

Université Libre de Bruxelles, Brussels, Belgium
Universidade Federal de Sao Paulo, Brazil
University of Turku, Turku, Finland
Université Paris Sud XI, Paris, France
University of Madras, Chennai, India
University Pavol Jozef Šafàrik, Kosice, Slovakia
Universidad Autonoma de Madrid, Centro de Investigaciones Oncologicas
(CNIO), Spain
Johns Hopkins School of Medicine, Baltimore, MD, USA
Johns Hopkins Krieger School of Arts and Sciences, Baltimore, MD, USA
National Institutes of Health, Bethesda, MD, USA
Ohio State University, Columbus, OH, USA
Albert Einstein College of Medicine of Yeshiwa University, N.Y., USA

Supporting Institutions

Ministero dell’Università e della Ricerca
Associazione Leonardo di Capua, Naples, Italy
Dipartimento di Biologia e Patologia Cellulare e Molecolare “L. Califano”,
Università degli Studi di Napoli “Federico II”, Naples, Italy
Istituto Superiore di Oncologia (ISO), Genoa, Italy
Università Italo-Francese, Torino, Naples, Italy
Università degli Studi di Udine, Udine, Italy
Agenzia Spaziale Italiana Istituto di Endocrinologia ed Oncologia Sperimentale
“G. Salvatore”, CNR, Naples, Italy

Italian Faculty

Giancarlo Vecchio, MD, Co-ordinator
Salvatore Maria Aloj, MD
Francesco Saverio Ambesi Impiombato, MD
Francesco Beguinot, MD
Maria Teresa Berlingieri, MD
Angelo Raffaele Bianco, MD
Bernadette Biondi, MD
Francesca Carlomagno, MD
Gabriella Castoria, MD
Angela Celetti, MD
Mario Chiariello, MD
Lorenzo Chiariotti, MD
Vincenzo Ciminale, MD
Annamaria Cirafici, PhD
Annamaria Colao, MD
Alma Contegiacomo, MD
Sabino De Placido, MD
Gabriella De Vita, MD
Jacques E. Dumont, MD
Monica Fedele, PhD
Pietro Formisano, MD
Alfredo Fusco, MD
Michele Grieco, MD

Massimo Imbriaco, MD
Paolo Laccetti, PhD
Antonio Leonardi, MD
Paolo Emidio Macchia, MD
Barbara Majello, PhD
Rosa Marina Melillo, MD
Claudia Miele, PhD
Francesco Oriente, MD
Roberto Pacelli, MD
Giuseppe Palumbo, PhD
Silvio Parodi, MD
Nicola Perrotti, MD
Giuseppe Portella, MD
Giorgio Punzo, MD
Antonio Rosato, MD
Massimo Santoro, MD
Martin Schlumberger, MD
Giampaolo Tortora, MD
Donatella Tramontano, PhD
Giancarlo Troncone, MD
Gilbert Vassart, MD
Giuseppe Viglietto, MD
Roberta Visconti, MD
Mario Vitale, MD

Foreign Faculty

***Université Libre de Bruxelles
(Belgium)***

Gilbert Vassart, MD
Jacques E. Dumont, MD

***Universidade Federal de Sao
Paulo, Brazil***

Janete Maria Cerutti, PhD
Rui Monteiro de Barros Maciel, MD
PhD

***University of Turku, Turku,
Finland***

Mikko Laukkanen, PhD

***Université Paris Sud XI, Paris,
France***

Martin Schlumberger, MD
Jean Michel Bidart, MD

***University of Madras, Chennai,
India***

Arasambattu K. Munirajan, PhD

***University Pavol Jozef Šafàrik,
Kosice, Slovakia***

Eva Cellárová, PhD
Peter Fedoročko, PhD

***Universidad Autonoma de Madrid -
Instituto de Investigaciones
Biomedicas (Spain)***

Juan Bernal, MD, PhD
Pilar Santisteban, PhD

***Centro de Investigaciones
Oncologicas (Spain)***

Mariano Barbacid, MD

***Johns Hopkins School of Medicine
(USA)***

Vincenzo Casolaro, MD
Pierre A. Coulombe, PhD

James G. Herman MD
Robert P. Schleimer, PhD

***Johns Hopkins Krieger School of
Arts and Sciences (USA)***

Eaton E. Lattman, MD

***National Institutes of Health,
Bethesda, MD, USA***

Michael M. Gottesman, MD
J. Silvio Gutkind, PhD
Genoveffa Franchini, MD
Stephen J. Marx, MD
Ira Pastan, MD
Phillip Gorden, MD

***Ohio State University, Columbus,
OH, USA***

Carlo M. Croce, MD
Ginny L. Bumgardner, MD PhD

***Albert Einstein College of
Medicine of Yeshiva University,
N.Y., USA***

Luciano D'Adamio, MD
Nancy Carrasco, MD

**Role of Pax8
transcriptional factor in
the differentiated
thyroid**

TABLE OF CONTENTS

ABSTRACT	8
1. BACKGROUND	9
1.1 The development of the thyroid in mice	9
1.1.1 The organogenesis of the thyroid	9
1.1.2 The differentiation of thyroid follicular cells	10
1.2 Genetically modified mice for the study of thyroid gland development	13
1.3 Pax8 in differentiated thyroid follicular cells	17
1.4 Conditional knock-out for the study of adult thyroid	18
1.4.1 Mouse strains already available used in this thesis	19
2. AIMS OF THE STUDY	22
3. MATERIALS AND METHODS	23
3.1 Targeting vector and Generation of Pax8 ^{fl/+} mouse	27
3.2 Mouse lines	27
3.3 ES cells screening	27
3.4 Mice screening	28
3.5 Histology, immuno-histochemistry and immune-fluorescences	30
3.6 Hormone measurements	31
3.7 RT-PCR and Quantitative Real-time PCR	31
3.8 Array hybridization and data analysis	32
3.9 Administration of Tamoxifen	33
4. RESULTS AND DISCUSSION	34
4.1 Generation of a conditional allele of the Pax8 gene	34
4.2 Cre-mediated recombination of floxed Pax8 allele: deletion of the floxed Pax8 allele mediated by Pax8-Cre (strain Pax8 ^{Cre/fl})	37
4.2.1 Thyroid morphogenesis in Pax8 ^{Cre/fl} mice	39
4.2.2 Analysis of the structure and function of the thyroid in Pax8 ^{Cre/fl} mice	42

4.2.3 Molecular phenotype of thyroid in Pax8 ^{Cre/fl} mice: gene expression analysis	46
4.2.4 Global gene expression profile in Pax8 ^{Cre/fl} thyroid mice	50
4.3 Cre-mediated recombination of floxed Pax8 allele: deletion of the floxed Pax8 allele mediated by Tg-Cre ^{ER}	55
CONCLUSIONS	63
REFERENCES	65

ABSTRACT

In Pax8^{-/-} mice the thyroid anlage disappears around E11.5. At birth the gland appears as a rudimentary structure composed only of C cells while thyroid follicular cells are undetectable. Thus, this model does not allow the study of Pax8 function in the postnatal thyroid.

To address the role of Pax8 in the differentiated thyroid, I established novel strains amenable to thyroid follicular cell-specific conditional knockout of Pax8 gene using the Cre/lox system. A genetically modified mouse strain (Pax8^{fl/fl}) harbouring a floxed allele of Pax8 was generated. These mice were crossed with two different Cre mice, a Pax8^{Cre/+} strain expressing constitutively Cre recombinase by embryonic day 8.5 and a Tg-Cre^{ER} strain in which Cre is active in thyroid follicular cells following tamoxifen injection.

Pax8^{Cre/fl} mice do not display an overt phenotype during embryonic life. However, 3-week old Pax8^{Cre/fl} pups show a hypothyroid phenotype characterized by both an increased serum TSH value and a significant reduction in body weight when compared with their wild type littermates. In Pax8^{Cre/fl} animals the thyroid gland is hypoplastic and shows the absence of the follicular structure; moreover, the expression of many thyroid specific genes, required for both hormone production and regulative functions, is completely abolished. In addition, survival of follicular cells is impaired.

The disruption of Pax8 in adult life (Pax8^{ko/fl};Tg-Cre^{ER} strain) seems to be not efficient and thyroid structure appears comparable to that of wild type. However, the absence of a clear phenotype in the Pax8^{ko/fl};TgCre^{ER} thyroid could be due to the compensatory proliferation of cells in which Pax8 has not been inactivated.

In conclusion, in my thesis work I demonstrated *in vivo* that Pax8 plays a key role in controlling both the expression of many thyroid specific genes and the survival of thyroid follicular cells.

1. BACKGROUND

1.1 The development of the thyroid in mice

1.1.1 The organogenesis of the thyroid

The thyroid gland, a component of the endocrine system, is responsible for producing thyroid hormone, known for its role in regulating metabolism in adults and is also required for many developmental processes.

The mammalian thyroid gland consists of two elongated lobes, connected by a very thin isthmus, located in front of the trachea, between the thyroid cartilage and the fourth tracheal ring. The thyroid parenchyma is composed of various epithelial cells. Thyroid follicular cells (TFCs), destined to produce thyroid hormones, are most abundant and are organized in particular spheroid structures known as follicles, each composed of a layer surrounding a closed cavity containing the colloid. TFCs are highly differentiated and express a number of proteins required for the synthesis and the release, in the blood, of thyroid hormones.

Both the final structure of thyroid and the differentiation of TFCs occur during embryonic life through a process, that in mice, starts around embryonic day (E) 8-8.5 and is completed by E16.5-17.

Thyroid anlage, the presumptive thyroid-forming district, is evident by E 8-8.5, as a midline thickening of the endodermal epithelium in the ventral wall of the primitive pharynx and is localized caudal to the so called tuberculum impar (Kaufman and Bard 1999), the region of the first branchial arch that gives rise to the median portion of the tongue. The thyroid anlage very shortly changes its appearance: the thickened bud first appears as a depression in the endodermal layer, evaginates from the floor of the pharynx and by E9 invades the surrounding mesenchyme. By E9.5-10 thyroid anlage appears as a flask-like structure that becomes a diverticulum and begins a caudal translocation towards its final position (Di Lauro and De Felice 2003) (Fig. 1). The migrating thyroid bud is connected to the pharynx by a narrow channel, the thyroglossal duct, a transient structure that regresses and is no longer visible by E11.5. On E12-12.5, the thyroid bud shows proliferation and grows laterally continuing its downward migration. At E13-14, the developing thyroid reaches its definitive pre-tracheal position and joins with the ultimobranchial bodies, which are the transient embryonic structures derived from the fourth pharyngeal pouch and contain the precursors of calcitonin-producing cells.

The two rudimentary para-tracheal lobes expand by E15-16 and the thyroid gland assumes its definitive shape. TFCs start organizing into cords of cells forming small rudimentary follicles. In the late fetal life, thyroid increases in size and its parenchyma is organized into small follicles, surrounded by a capillary network, enclosing thyroglobulin in their lumen. At birth, thyroid gland is able to produce and release thyroid hormones through the regulation of

its growth and function by the hypothalamic-pituitary axis is fully active only after birth (De Felice et al. 2004).

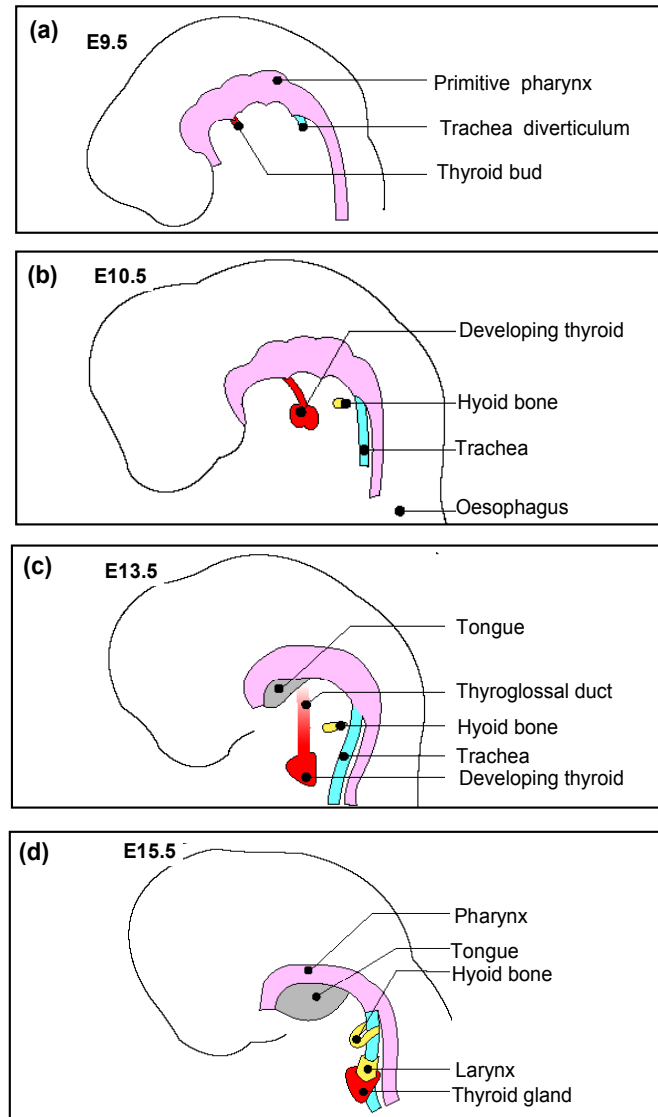


Figure 1 Development of thyroid in mouse. (a) Formation of the thyroid bud and diverticulum. (b) The developing thyroid extends caudally forming the thyroglossal duct which (c) disappears as the thyroid reaches its destination. (d) The thyroid gland in situ. The developmental stage is indicated in embryonic (E) day.

(From Di Lauro and De Felice 2003)

1.1.2 The differentiation of thyroid follicular cells

As soon as the thyroid anlage is visible as an endodermal thickening in the midline of the floor of the primitive pharynx, the precursors of TFCs acquire a specific molecular signature and can be distinguished by the co-expression of four transcription factors Hhex (Thomas et al. 1998), Titf1 (Lazzaro et al.

1991), Pax8 (Lazzaro et al. 1991) and Foxe1 (Zannini et al. 1997). It is worth noting that each of these transcription factors is expressed also in other tissues but such a combination is a unique hallmark of both differentiated thyroid follicular cells and their precursors (Damante et al. 2001). Studies in animal models have shown the relevance of these factors for thyroid development. In the absence of either Titf1, Hhex, Pax8 or Foxe1 the thyroid anlage is correctly formed but the subsequent thyroid morphogenesis is severely impaired (Parlato et al. 2004). The presence of Titf1 (Kimura et al. 1996; Kimura et al. 1999), Hhex (Martinez Barbera et al. 2000) and Pax8 (Mansouri et al. 1998) is required for the survival of the TFC precursors, whereas in the absence of Foxe1 the thyroid primordium either disappears or remains in a sub-lingual ectopic position (De Felice et al. 1998). These data indicate that Titf1, Hhex, Pax8 and Foxe1 play individual roles in the organogenesis of the gland; however functional interaction among these factors has been demonstrated in developing thyroid (Fig. 2).

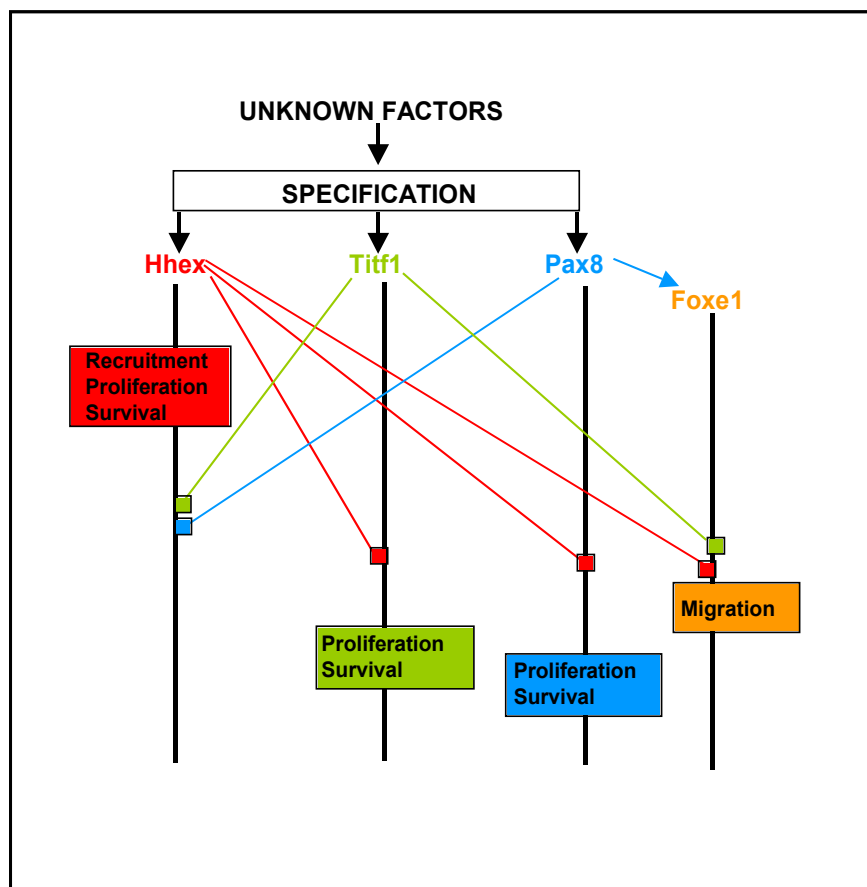


Figure 2 Functional interactions among Hhex, Titf1, Pax8 and Foxe1 in developing thyroid. The transcription factor and the functions controlled by it are indicated in different colours. Each factor regulates other transcription factors controlling the onset (arrow) or the maintenance (square) of their expression.

(From Parlato et al. 2004)

Actually, *Titf1*, *Hhex* and *Pax8* are linked in a complex regulatory network because each of them controls the maintenance of expression of the other factors. The simultaneous presence of these three factors is required for the expression of *Foxe1*, suggesting that *Foxe1* is located downstream in the thyroid regulatory network (Parlato et al. 2004).

Shortly after specification, TFC precursors begin to translocate to reach the sub-laryngeal position, a process that lasts for almost four days. The expression of transcription factors such as either *Hhex* or *Pax8* or *Titf1* is not sufficient for thyroid migration, while *Foxe1* plays a crucial role because the presence of this factor in the thyroid bud is required to allow the cells to move (De Felice et al. 1998; Parlato et al. 2004). Thus, in TFC precursors, *Foxe1* is likely to control the expression of key molecules required for migration, though it has been suggested that the translocation of thyroid primordium towards the sub-laryngeal position not only depends on cell autonomous events but could also be driven by the movements of other surrounding tissues of the neck region (Hilfer and Brown 1984).

When the thyroid primordium reaches the sub-laryngeal position, TFC precursors accomplish their functional differentiation and the gland acquires its definitive shape, two lobes connected by an isthmus. The process leading to the formation of the two lateral lobes of the gland seems to be controlled by inductive signals originating from adjacent structures, mainly the vessels located close to the thyroid tissue. This is observed in mice in which, when either Sonic hedgehog (*Shh*) (Fagman et al. 2004) or *TBX1* (Fagman et al. 2006) has been disrupted, correct patterning of the vessels is disturbed; the lobulation process is impaired and the thyroid gland assumes the shape of a single midline mass located lateral to the trachea.

The final differentiation of TFC is featured by the expression of a number of genes required for thyroid function such as thyroglobulin (*Tg*), thyroid peroxidase (*TPO*), TSH receptor (*Tshr*); sodium/iodide symporter (*NIS*), thyroid oxidases (*Thox*'s) and pendrin (*PDS*). The final differentiation program of TFC requires almost three days. *Tg* appears around E14 (Lazzaro et al. 1991) while thyroxine is first detected at E16.5 (Meunier et al. 2003). The expression of both *TPO* and *NIS*, the two key enzymes involved in the process of *Tg* iodination, is absolutely dependent on the pathway activated by the binding of TSH to its receptor, *Tshr* (Postiglione et al. 2002). It is worth noting that in mice, this pathway is not much relevant for the expansion of the fetal thyroid; in contrast, the growth of adult thyroid is dependent on TSH/*Tshr*/cAMP signals (De Felice et al. 2004). Thus, some characteristics are acquired by TFCs only after birth.

1.2 Genetically modified mice for the study of thyroid gland development

In recent years, genes and mechanisms involved in thyroid morphogenesis have been partially identified. These findings are due to studies on murine models generated in gene targeting experiments.

Gene targeting in mice allows defined modifications, such as deletions, insertions, and point mutations, to be made at specific points in the mouse genome. This is achieved in cells by homologous recombination of a targeting vector that contains the desired change (Thomas and Capecchi 1987). This is normally carried out in embryonic stem (ES) cells as these cells have high rates of homologous recombination and are able to contribute to the germline when re-introduced into mouse embryos at the morula or blastocyst stage of development (van der Weyden et al. 2002; Bradley A 1991; Bradley A 1993). The generation of murine strains in which thyroid relevant genes have been disrupted has provided useful animal models to study the genetic mechanisms of thyroid development. In addition, these models have been valuable in elucidating the molecular pathology of thyroid dysgenesis, the most frequent cause of congenital hypothyroidism.

Hhex knock-out mice

During development Hhex is also expressed in the primordium of several organs derived from the foregut, including thyroid bud. Hhex is an early marker of thyroid cells, since it is present in the thyroid anlage at E 8-8.5 (Thomas et al. 1998) at the same stage in which *Titf1*, *Foxe1* and *Pax8* are detected. The analysis of *Hhex*^{-/-} embryos has revealed that this factor is absolutely necessary for thyroid morphogenesis (Martinez-Barbera et al. 2000). In *Hhex* null embryos, at E8.5, TFCs are present in the anterior wall of the pharynx (Parlato et al. 2000). One day later the thyroid primordium is absent or hypoplastic and the thyroid precursor cells do not express *Titf1*, *Foxe1* and *Pax8* (Martinez-Barbera et al. 2000). Hence at early stages of development, the presence of Hhex could be required to maintain the expression of *Titf1*, *Foxe1* and *Pax8* in the thyroid primordium.

Titf1 knock-out mice

Titf1 (or *Nkx2-1*) was initially identified in a rat thyroid cell line (Civitareale et al. 1989) as a nuclear protein able to bind to specific sequences in the Tg promoter.

Titf1 is expressed in both differentiated follicular cells and in their precursors. It is detected in the thyroid primordium as soon as the thyroid anlage is visible. In the thyroid gland, *Titf1* expression is not restricted to the follicular cells; it is also present in parafollicular C-cells (Suzuki et al. 1998). In addition, *Titf1* is

expressed in selected areas of the forebrain, including the developing posterior pituitary, in the trachea and in the lung epithelium (Lazzaro et al. 1991).

Gene targeting experiments have allowed the study of the role of this transcription factor during embryonic life. Mice, in which both *Titf1* alleles have been disrupted, show a complex phenotype according to the wide expression domain of this gene.

In absence of *Titf1*, the newborn mice immediately die at birth and are characterized by impaired lung morphogenesis, lack of thyroid (Fig.3) and pituitary and severe alterations in the ventral region of the forebrain (Kimura et al. 1996)

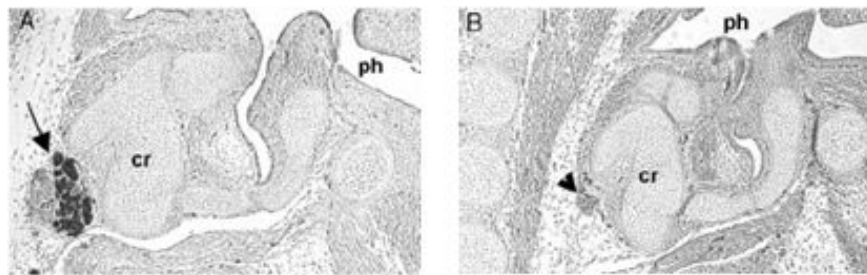


Figure 3 Sagittal sections of wild-type (A) and *Titf1*^{-/-} (B) E15.5 embryos stained with Pax8 antibody. In wild-type embryo, the developing thyroid (arrow) is positioned dorsal to the cricoid cartilage. In the mutated embryo the thyroid tissue is undetectable (arrowhead). Cr: Cricoid cartilage; ph: pharynx (De Felice and Di Lauro 2004).

Analyses during development demonstrate that the thyroid anlage forms in its correct position but at an early stage, morphogenesis of the gland is impaired. The thyroid primordium by E10.5 appears much smaller in size in comparison to wild type and subsequently undergoes degeneration probably in consequence of an apoptotic process (Kimura et al. 1996). Hence, *Titf1* is dispensable for the initial commitment of thyroid cells, but is required for the survival and subsequent differentiation of the cells. However, we do not know which genes are controlled by this transcription factor in the thyroid primordium.

Pax8 knock-out mice

Pax8 is expressed in adult and developing thyroid since the early stages of gland morphogenesis. In addition, *Pax8* is initially but transiently expressed in the myelencephalon and through the entire length of the neural tube during embryonic life (Plachov et al. 1990) and is present in the developing kidneys, where it is maintained throughout adult life.

Analysis of *Pax8*^{-/-} mice (Mansouri et al. 1998) offers the possibility of studying the role of this transcription factor in embryonic life. *Pax8* null pups show growth retardation and die within 2-3 weeks of their birth. The animals

are affected by a severe hypothyroidism and present a rudimental gland composed almost completely of calcitonin-producing C cells while the TFCs are absent (Fig. 4). In Pax8 null embryos the thyroid anlage forms, evaginates from the endoderm and begins to migrate into the mesenchyme. However by E11 the thyroid bud is smaller in comparison to that of wild type. In addition, other transcription factors, such as Foxe1 and Hhex, are down-regulated in the precursors of thyroid cells in the absence of Pax8 (Parlato et al. 2000). Finally, by E12.5 TFC is not detectable (Mansouri et al. 1998).

Thus, during morphogenesis, Pax8 holds a specific upper role in the genetic regulatory cascade that controls thyroid development and it is required for the survival of the TFCs and to maintain the tissue-specific gene expression program.

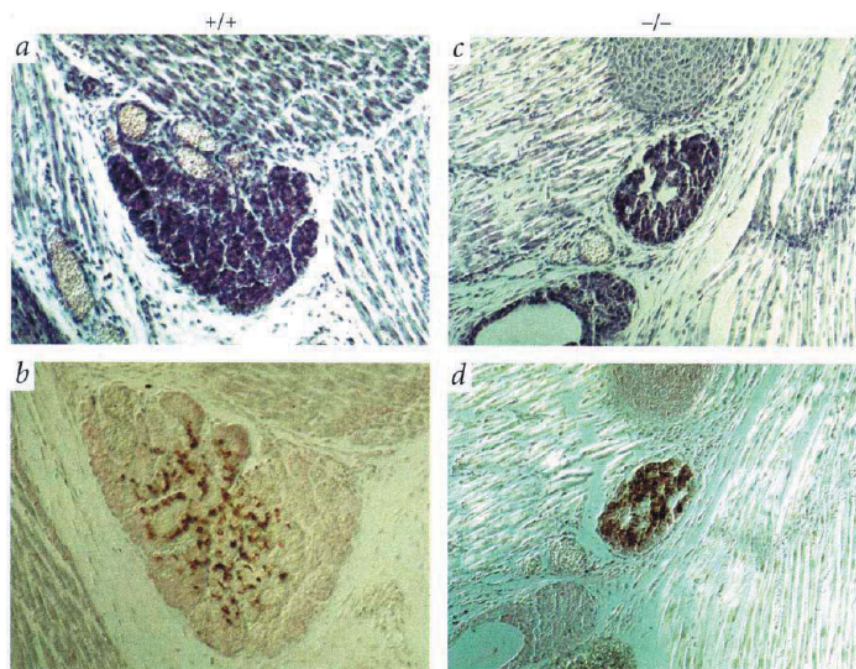


Figure 4 Analysis of calcitonin-producing cells in the thyroid gland of Pax8^{-/-} mouse embryos. Sagittal sections control embryos (a,b) and Pax8^{-/-} embryos (c,d) stained with haematoxylin/eosin (a,c) and immunohistochemistry using anti-calcitonin antibody (b,d). (Mansouri et al. 1998)

Foxe1 knock-out mice

Foxe1 was originally identified as a thyroid specific nuclear protein that can bind to a sequence present on both Tg and TPO promoters under insulin, IGF-1 or TSH stimulation (Santisteban et al. 1992).

Foxe1 is detected in the thyroid primordium and its expression is maintained in TFCs during all stages of development and in adulthood. During embryonic life, it has a wide domain of expression. Indeed, at early stages of development, Foxe1 is detected in the endodermal epithelium lining the primitive pharynx, the arches and the foregut and transiently in the Rathke's pouch. Subsequently

Foxe1 is expressed also in the tongue, in the secondary palate, in the definitive choanae, and in the whiskers and hair follicles (Dathan et al. 2002). Analysis of Foxe1 null mice revealed the role of this transcription factor in thyroid development. Targeting inactivation of Foxe1 shows that homozygous Foxe1^{-/-} mice are born at the expected Mendelian ratio but die within 48 hours. These mice display a severe cleft palate, probably responsible for the prenatal death, no thyroid in its normal location, absence of thyroid hormones and elevated TSH levels in the bloodstream (De Felice et al. 1998). In Foxe1^{-/-} embryos, at early stages of thyroid morphogenesis, the formation of the thyroid anlage is not affected. However, at E10 in Foxe1 null embryos, TFCs are still on the floor of the pharynx whereas in wild type embryos the thyroid primordium begins to descend towards its final location.

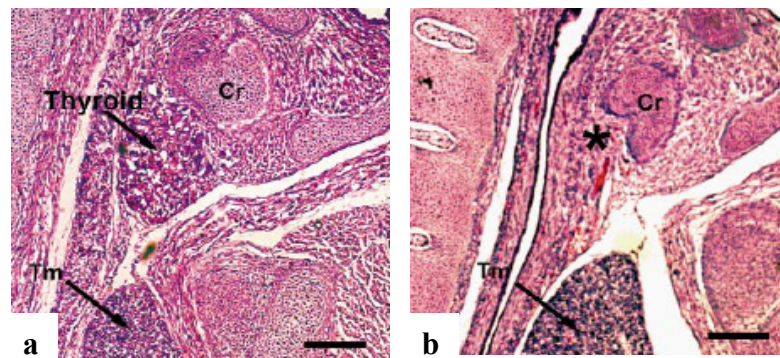


Figure 5 Analysis of Foxe1^{-/-} newborn phenotype. Sagittal sections through the thyroid region of Foxe1^{+/-} (a) or Foxe1^{-/-} (b) mice. Thyroid is adjacent to cricoid cartilage in normal mouse and absent (*) in homozygous mouse. (De Felice et al. 1998)
ps, palatal shelves; Cr, cricoid cartilage; Tm, thymus.

At later stages of development, in the absence of Foxe1, TFCs either disappear (Fig.5) or form a small thyroid remnant still attached to the pharyngeal floor. In this case, the cells are able to go on their differentiative program as tested by the synthesis of thyroglobulin. These data indicate that in embryonic life Foxe1 has a specific role in controlling the migration of TFC precursors, but is not relevant for the specification and differentiation of the thyroid anlage. In addition, Foxe1 could be involved in the survival of TFCs since in many Foxe1 null embryos the thyroid primordium disappears (De Felice et al. 1998; Parlato et al. 2004).

Tshr knock-out mice

Tshr (thyroid stimulating hormone receptor) is detected in TFC precursors by E14-14.5 (Lazzaro D et al. 1991; Brown RS et al. 2000). At later stages of development Tshr expression increases and remains expressed in adult life. The role of TSH/Tshr signaling in vivo during embryonic life has been studied in genetically modified mice in which Tshr gene has been disrupted by

homologous recombination (*Tshr*^{-/-}) mice (Marians RC et al. 2002). E16 mouse embryos deprived of TSH/*Tshr* signaling do not show defects in morphology of the gland which displays a normal size and follicular structure though both TPO and NIS are undetectable in TFCs (Postiglione MP et al. 2002). During thyroid morphogenesis TSH pathway is absolutely required for the differentiation process of the thyroid but it does not appear to be relevant for the growth of the gland. On the contrary, adult *Tshr*^{-/-} mice display a severe hypoplastic adult thyroid (Marians RC et al. 2002; Postiglione MP et al. 2002).

1.3. Pax8 in differentiated thyroid follicular cells

Pax8 is a paired domain containing transcription factor and belongs to the Pax family of transcription factors. In mice Pax8 gene is split in 12 exons (Okladnova O et al. 1997); alternative splicing produces transcripts that differ in their carboxy-terminal regions. It has been demonstrated that the expression of different isoforms is temporally and spatially regulated during early mouse development. Furthermore PAX8 isoforms display different trans-activating activities when tested in cell lines.

In *Pax8* null mice mature TFCs are absent making it difficult to reveal the role of this factor in the control of adult thyroid function. All the available data on Pax8 functions in differentiated cells, come from studies on cell lines in culture. Consensus sequences recognized by Pax8 have been found in the proximal promoters of *Tg* and *TPO* and in an upstream enhancer of *NIS* (Ohno M et al. 1999). In both *Tg* and *TPO* proximal promoters, Pax8 binding sites partially overlap Titf1 binding sequences (Zannini MS et al. 1992); in *NIS* enhancer the two Pax8 sites flank a cAMP response element and recently it has been shown that Pax8 is able to bind *in vitro* to the 5-flanking region of *Foxe1* and *ThOX2* genes (D'Andrea B et al. 2006).

Functional assays carried out in non thyroid cell lines have demonstrated that Pax8 is required to activate the *TPO* promoter and to a less extent the *Tg* promoter (Zannini MS et al. 1992) and *NIS* enhancer (Ohno M et al. 1999). In addition, it has been demonstrated that in transformed thyroid cells Pax8 is sufficient to activate expression of the endogenous genes encoding *Tg*, *TPO* and *NIS*. These data suggest that Pax8 has an important role in the maintenance of functional differentiation in thyroid cells (Pasca di Magliano M et al. 2000). It is worth noting that Pax8 is expressed together with Titf1 only in TFCs. Both of them bind to sequences present in the regulative regions of thyroid specific genes; furthermore the Pax8 binding site overlaps with the Titf1 binding site on both *Tg* and *TPO* promoters (Zannini MS et al. 1992). These findings suggest some interaction between Titf1 and Pax8. In fact co-immunoprecipitation experiments in thyroid cells have shown that Titf1 and Pax8 form *in vivo*, a protein complex, which is probably mediated by protein-protein interaction since it does not require the binding to DNA (Di Palma et al. 2003). Titf1 and Pax8 have also functional interactions, since the two factors cooperate in a

synergistic manner in activating Tg promoter. This functional interaction is mediated by the N-terminal domain of Titf1 and the C-terminal part of Pax8. It is worth noting that the synergistic effect of Titf1 and Pax8 is manifested on the minimal region of Tg promoter while it is not effective on TPO minimal promoter (Di Palma et al. 2003). In addition to the synergistic cooperation between Pax8 and Titf1, Pax8 can interact with other proteins which can be responsible for the target preferences in definite cell types or developmental stages. Assays *in vitro* have indicated a potential interaction between Pax8 and WBP-2, a protein containing a WW domain, a 40 amino acid long sequence involved in protein interactions (Nitsch R et al. 2004). WBP-2 is an ubiquitous protein but an alternatively spliced isoform of this protein seems to be expressed only in thyroid. Though the interaction between Pax8 and WBP-2 is found to be effective also *in vivo* there is no proof that the transcriptional activity of Pax8 is modulated in consequence to this interaction.

1.4. Conditional knock-out for the study of adult thyroid

Germline disruption of many genes results in early prenatal or even early embryonic death. In other cases the development of the organ of interest is blocked at an early stage thus preventing the study of late events of the morphogenesis. This is the case of the already generated thyroid mouse models. In Titf1, Foxe1, Hhex and Pax8 null mice the thyroid disappears at an early stage (around E11); it is impossible to study the role of some of these genes in the differentiated follicular cells and in the physiology of the gland. Hence, it is important to generate models in which the gene of interest is disrupted in both a specific stage and a specific tissue.

These problems can be resolved by conditional gene deletions which make use of the properties of recombinases to recognise specific target sequences that can be introduced into genomic DNA. The most common system used in mice is the Cre/loxP system (Hoess RH et al. 1982) (Fig. 6).

This makes use of the P1 bacteriophage Cre recombinase that recognises loxP sites, a 34 bp sequence that comprises two 13-bp inverted repeats flanking an 8 bp spacer region (Fig. 6a). This 8 bp sequence confers directionality on the loxP site; if two loxP sites are present in opposite orientations in a DNA sequence, Cre will catalyse the inversion of the intervening sequence. If both loxP sites are present in the same orientation then Cre will catalyse the removal of the intervening sequence (Fig. 6 c,d).

For conditional deletions, the gene of interest is modified to introduce loxP sites in the intron 5' and 3' to a selected group of exons that are essential to the function of the gene. These loxP sites do not interfere with the transcription of the gene, so the mice with this modified allele should be normal. If, however, Cre is expressed in the cells of these mice, the exons between the loxP sites will be deleted, resulting in a knock-out allele.

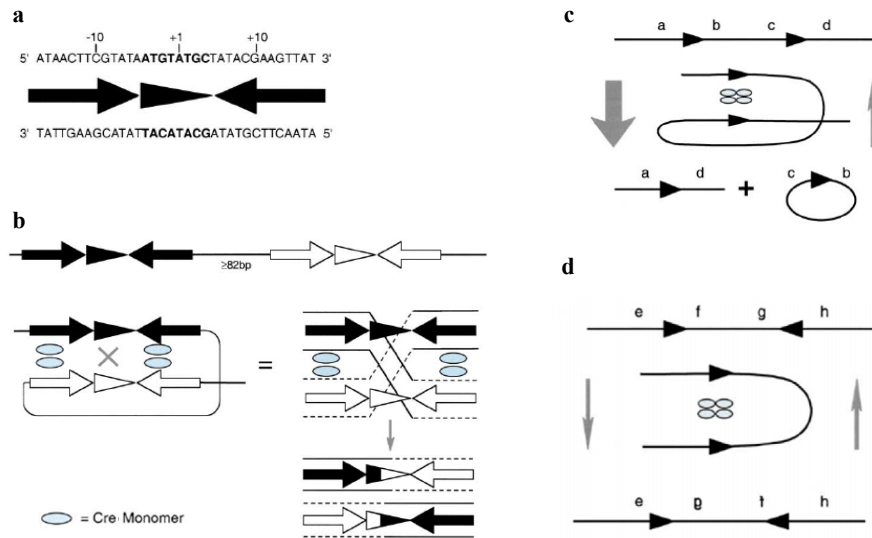


Figure 6 Cre target site and mechanism of the Cre-mediated recombination. (a) Cre recombinase target site, horizontal arrows mark the inverted repeats and the triangle the spacer; (b) Synaptic complex formed between recombinase molecules and two identical target sites. One recombinase monomer binds each 13 bp repeat, while the spacer sequence provides the site of strand cleavage, exchange (via a Holliday intermediate) and ligation. In the final product, there is an exchange of DNA between the two starting sites.

Cre expression can be achieved using viruses, although the most common method is to cross the mice to a Cre-expressing strain. Many Cre-expressing mouse models have been made, including ones which express Cre under the control of inducible or tissue specific promoters, thereby allowing control of where and when the deletion occurs.

1.4.1 Mouse strains already available used in this thesis

In my thesis work I used two different Cre-driver mice, a Pax8^{Cre/+} (Bouchard et al, 2004) and a Tg-Cre^{ER} strain, both already available in the laboratory. The Pax8-Cre mouse is a knock-in model obtained by inserting a *cre* gene in-frame into Pax8 exon 3 (Fig. 7a), in this way the expression pattern of the recombinase reflects that of the Pax8 gene (Fig. 7b), in fact it starts to be detected at E8,5 in the thyroid gland, inner ear, kidney and in the mid-hindbrain boundary region.

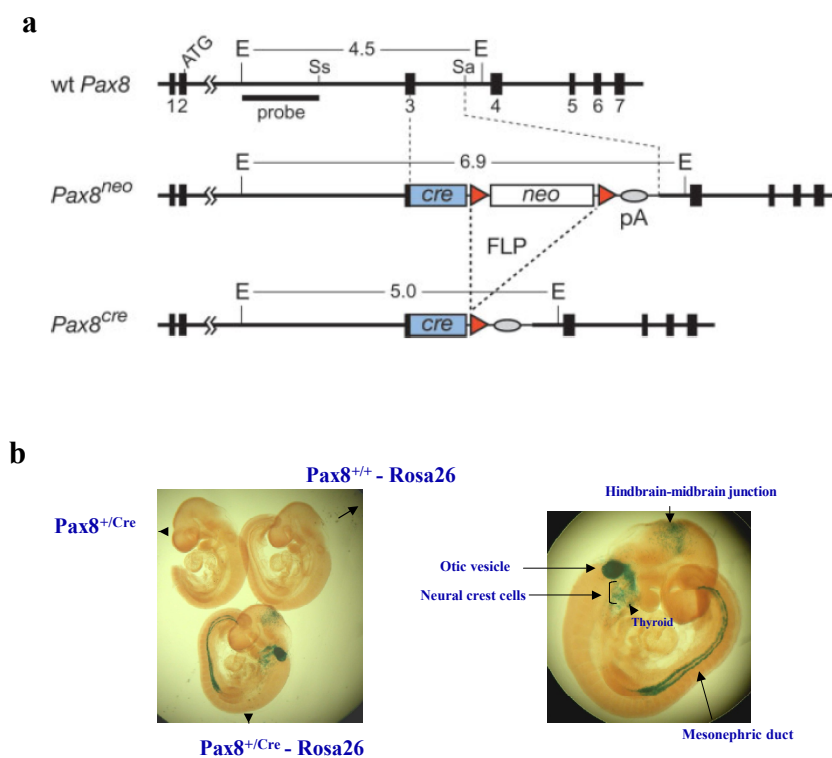


Figure 7 Generation of the Pax8-Cre mouse. (a) Structure of wild-type and mutant Pax8 alleles; (b) β -Galactosidase assay on embryo at E9.5 obtained by crossing Pax8^{Cre/+} mice with Rosa26-LacZ mouse. Rosa 26-LacZ is a knock in mouse expressing the reporter gene LacZ under the control of the ubiquitous promoter Rosa26

The Tg-Cre^{ER} strain is a transgenic mouse model in which a Cre, under the control of the thyroglobulin promoter, has been fused to a mutated form of the ligand binding domain of the estrogen receptor. The mutant ER does not bind its natural ligand at physiological concentrations, but binds to a synthetic ligand, tamoxifen. Thus, CreER activity can be induced following tamoxifen injection, thereby allowing the temporal deletion of the loxP flanked gene (Fig. 8).

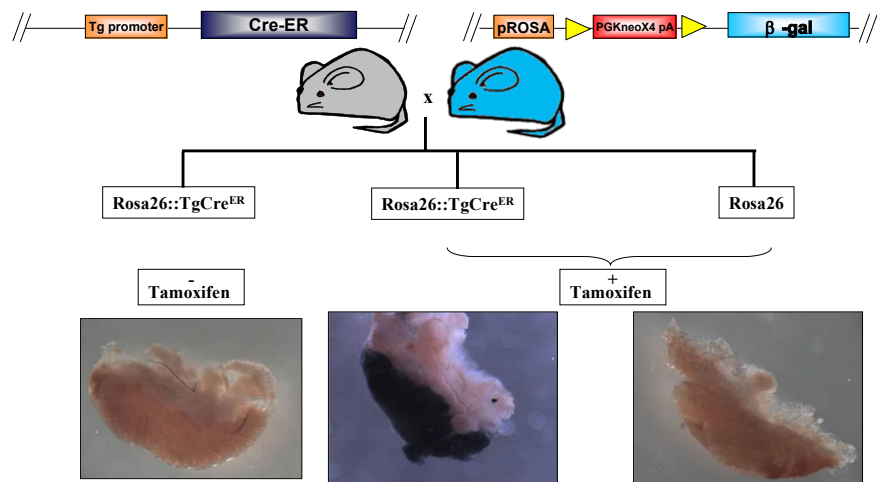


Figure 8 β -Galactosidase assay performed on adult thyroids of Rosa26-LacZ::TgCre^{ER} mice. Only when the mice are injected with tamoxifen the Cre recombinase is active and the reporter gene is expressed.

2. AIMS OF THE STUDY

Pax8 is absolutely required for the development of the thyroid. Thanks to an animal model (Pax8^{-/-} mice) we know that this transcription factor controls the survival of thyroid precursor cells. However, In Pax8 null mice mature thyroid follicular cells are absent, making it difficult to reveal the role of this factor in the adult thyroid.

Experiments in thyroid cell lines have shown that Pax8 has an essential role in the maintenance of the phenotype of thyroid follicular cells, controlling the expression of several thyroid specific genes, essential for the production of thyroid hormones. Pax8 activates the expression of the endogenous genes encoding *Tg*, *TPO* and *NIS* at their chromosomal locus. Furthermore, in thyroid transformed cell lines re-activation of Pax8 expression can restore a differentiated thyroid phenotype.

Despite of the essential role played by Pax8 in thyroid follicular cells, we do not have any animal models to study the role of this factor *in vivo*; all the available data on Pax8 functions in differentiated cells come from studies on cell lines in culture. Sometimes, studies in cell lines may not be an exhaustive model for the understanding of the complex role of a transcription factor *in vivo*.

The aim of my thesis is to contribute to the study of Pax8 in the physiology of the thyroid gland by generating and analyzing the phenotype of a novel genetically modified mouse strain in which it is possible to disrupt the Pax8 gene in a controlled manner.

The availability of mouse strains expressing Cre recombinase in thyroid cells has allowed me to use a strategy based on the Cre/lox system to accomplish my goal.

3. MATERIALS AND METHODS

3.1 Targeting vector and Generation of Pax8^{fl/+} mouse

To design of Pax8 conditional knock-out (cKO) allele we considered two main objectives:

- 1) a pair of loxP sites must be inserted into intron regions of the target gene such that the encoded protein is inactivated through Cre-mediated excision of the loxP-flanked exons;
- 2) the target gene should not be disrupted by the presence of the loxP sites prior to Cre-mediated recombination. Hence, we decided to flank the exons 3 and 4 of Pax8, since they codify for the DNA binding domain, essential for the transcription factor functionality.

To generate the construct, we used the recombineering, or Red/ET recombination, method, a technique that allows for the insertion, deletion, or mutation of DNA sequences, assuaging the need for conveniently located restriction sites. By this method, the target DNA molecules are precisely altered by homologous recombination in strains of *E. coli* which express three phage proteins, Gam, Beta and Exo, which are collectively called Red proteins (Zhang et al 1998, Copeland et al 2001, Court et al 2002). The Gam protein inhibits RecBCD and SbcCD exonuclease activities of *E. coli*, thus preserving linear dsDNA and allowing it to be used as a substrate for recombination (Sawitzke et al 2007); Beta protein is a single-stranded DNA (ssDNA)-binding protein that promotes annealing of complementary DNA strands (Court et al 2002, Mythili 1996). Beta can bind stably to ssDNA longer than 35 nucleotides and can protect ssDNA overhangs from single-strand nuclease degradation. Exo is a dsDNA-dependent 5'-3' exonuclease that processes linear dsDNA and generates a 3' ssDNA overhang at each end, the substrate that Beta protein binds (Cassuto E 1971). A functional interaction between Exo and Beta is required in order to catalyse the homologous recombination reaction.

In figure 9 the mechanism of Red/ET recombination is illustrated. Recombination occurs through homology regions, which are stretches of DNA shared by the two molecules that recombine.

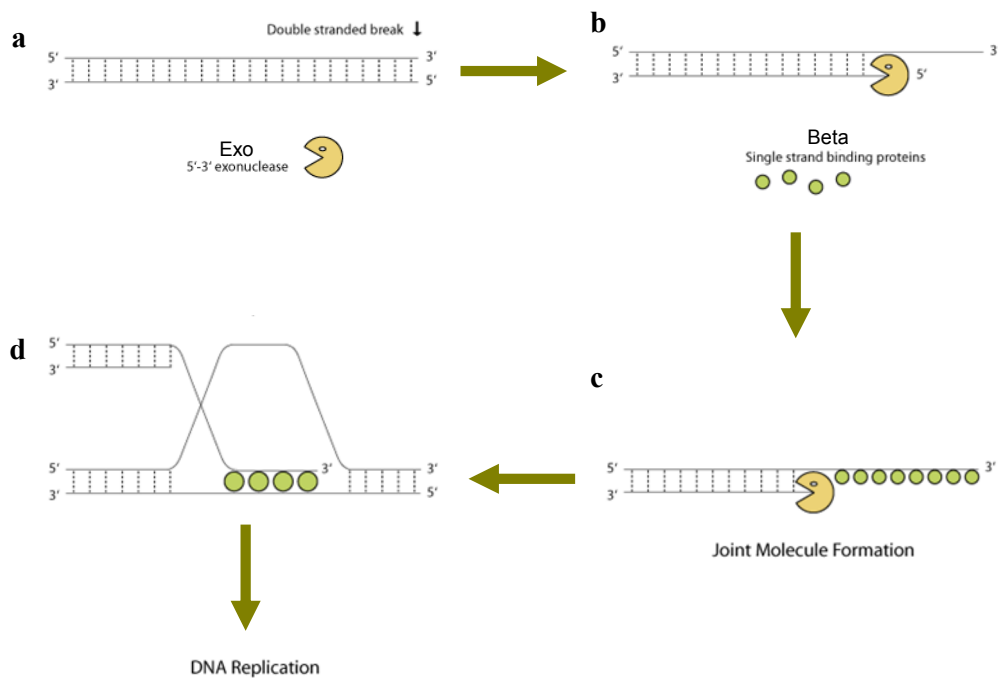


Figure 9 Mechanism of Red/ET recombination. (a) a double-stranded-break (DSB) repair is initiated by Exo; (b,c) first Exo degrades the DNA in a 5'-3' direction, starting from the DSB, thereby creating a 3' ssDNA overhang; (d) Beta binds to the ssDNA forming a recombinogenic proteonucleic filament which is used in recombination, either by single strand annealing or by strand invasion.

A double-stranded break repair is initiated by the recombinase protein, Exo, that digests one strand of the DNA from the double-stranded break, leaving the other strand as a 3' ended, single-stranded DNA overhang. Then Beta binds and coats the single strand and the protein-nucleic acid filament aligns with homologous DNA. Once aligned, the 3' end becomes a primer for DNA replication.

Using this technique, it is possible to target and modify, by insertion or deletion, any DNA sequence.

The process of generating the Pax8 conditional knock-out targeting vector was consisted of three main steps:

- 1) retrieval of genomic region of interest from a bacterial artificial chromosome (BAC) onto targeting vector backbone by gap repair;
- 2) insertion of an orphan loxP site;
- 3) insertion of FRT-neo-FRT-loxP cassette with the same orientation of the orphan loxP site.

Retrieval of genomic region of interest from a BAC onto targeting vector backbone

The BAC chosen to generate the Pax8 cKO targeting vector, bMQ241m1 (The Wellcome Trust Sanger Institute, Hinxton, UK), derive from a mouse 129Sv

genomic DNAs library, that is isogenic with the genomic DNA of the ES cells used for the homologous recombination, R1 (Nagy Basic ES cell line R1 129 strain); in this way the efficiency of homologous recombination is increased. To retrieve the genomic region of interest from the BAC, a couple of primers of 70 bp in length was designed to amplify by PCR the pBluescript II KS - (Stratagene) backbone. These primers consist of two parts, 20 bp at the 3' end, that is useful for the amplification of pBS, and 50 bp at 5', that represents the homology arm designed to mediate the recombinering (Fig. 10).

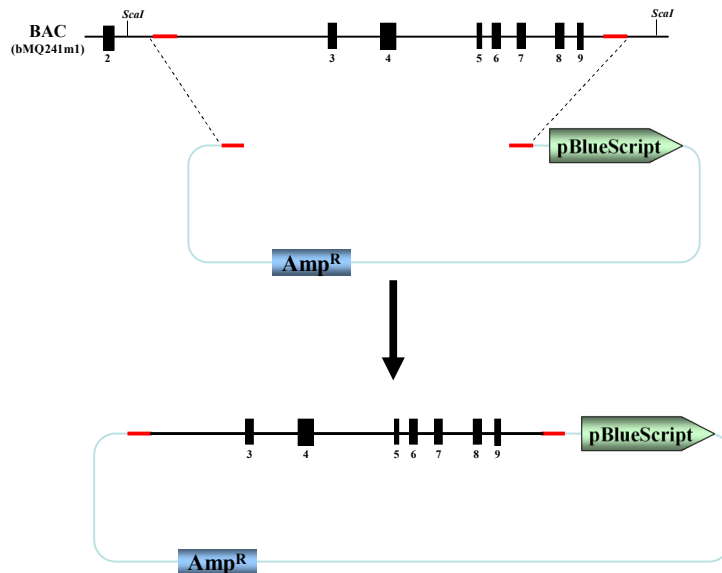


Figure 10 Retrieval of the gene sequence from the BAC by gap repair. The pBluescript backbone was amplified by PCR and the resulting product was a linear plasmid with 50 bp in length homology arms (*thin red layer*) at both ends, that are able to mediate the retrieving of the genomic sequence of interest from the BAC by gap repair. The positive bacterial clones were selected by ampicillin resistance. *Black boxes* indicate the coding regions, the exons are numerated. *Amp^R*, ampicilline-resistance cassette.

Insertion of an orphan loxP site

To insert the loxP orphan site, a second couple of primers, 70 bp in length, was designed to amplify a *loxP-neo-loxP* cassette from the pL452 plasmid (from National Cancer Institute – Frederick). Each primer was composed of 50 bases homologous to the region that is going to be targeted, and 20 bases homologous to the flanking regions of *loxP-neo-loxP* cassette; this allow the insertion of *loxP-neo-loxP* cassette, with screening in bacteria using kanamycin. To remove the *neo* cassette and leave an orphan loxP site, a Cre recombinase-mediated reciprocal recombination of loxP sites was carried out in bacterial strains (Fig. 11).

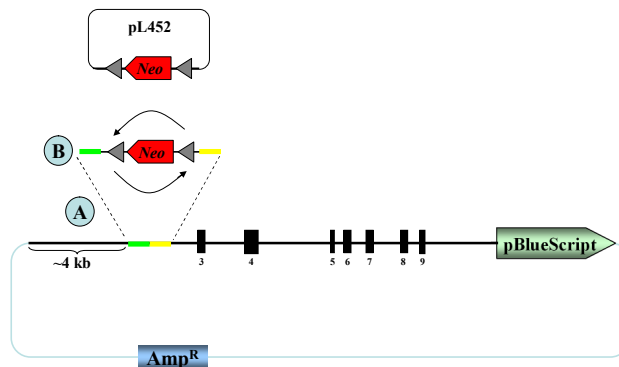


Figure 11 Insertion of an orphan loxP site. (A) loxP-Neo-loxP cassette was amplified by PCR, adding in the same time the 50 bp homology arms at both ends of this cassette (green and yellow thin layers). Recombination between homologous regions allows to insert the loxP-Neo-loxP cassette. The positive clones were selected by kanamycin resistance; (B) bacteria containing the retrieved genomic region with the loxP-Neo-loxP cassette were electroporated with a Cre-expressing plasmid, Cre-mediated recombination generates an orphan loxP. Black boxes indicate the coding regions, the exons are numerated. Amp^R, ampicilline-resistance cassette. Grey triangles indicate loxP sites, the red box represent the neo-resistant cassette.

Insertion of FRT-neo-FRT-loxP cassette

For this step, the same principle used for the insertion of the loxP-neo-loxP was followed (Fig. 12).

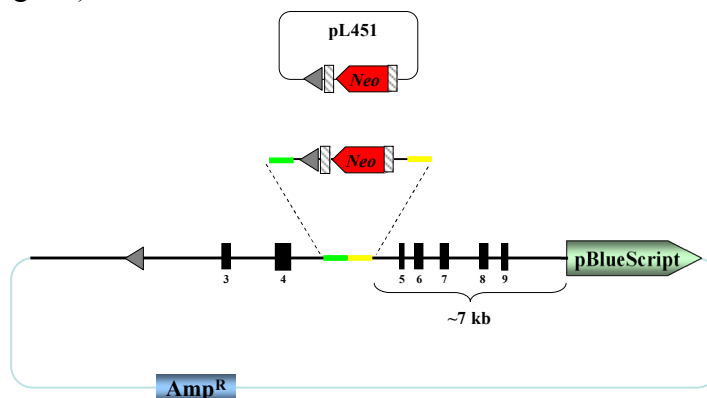


Figure 12 Insertion of a FRT-neo-FRT-loxP cassette. FRT-Neo-FRT-loxP cassette was amplified by PCR, from the pL451 plasmid (from National Cancer Institute – Frederick) adding in the same time the 50 bp homology arms at both ends of this cassette (green and yellow thin layers). Recombination between homologous regions allows to insert the FRT-neo-FRT-loxP cassette. The positive clones were selected by kanamycin resistance. Black boxes indicate the coding regions, the exons are numerated. Amp^R, ampicilline-resistance cassette. Grey triangles and shadow boxes indicate loxP sites, respectively; the red box represent the neo-resistant cassette.

Electroporation of the targeting vector in the ES cells

The R1 ES cells were maintained in Dulbecco's Modified Eagle's Medium (DMEM) supplemented with 15% FBS (EuroClone), 1/100 L-glutamine (Invitrogen), 1/100 NEAA (Invitrogen), 1/100 penicillin/streptomycin, 500 U/mL (Invitrogen), 1/500 2-mercaptoethanol, 1/10000 Lif (EuroClone) and

1/100 Na pyruvate. They were electroporated with the linearized targeting vector DNA using the MicroPorator MP-100 Digital Bio.

G418-resistant ES clones were selected, expanded and analyzed by PCR for detection of homologous recombinant, as described in Results and Discussion. The correctly targeted ES cells were electroporated with a FLP-expressing plasmid, pCAGGS-FlpeIRESPURO, to delete the pGK-Neo cassette by recombination between the FRT sites. Neomycin gene deletion was confirmed by PCR and the ES clones positive at this screening were injected into C57BL/6 blastocysts to generate chimeric founder mice as previously described (Hogan et al. 1994, Joiner 1993). Chimeric founder male mice were bred with C57BL/6 females. The germline-transmitted F1 mice were further crossed with Pax8 heterozygous mice (ko/+ and Cre/+), and with Tg-Cre^{ER} transgenic mice to generate all the mice used for the several experiments.

3.2 Mouse lines

Heterozygous Pax8-Cre mice (Pax8^{Cre/+}) were obtained from the Meinard Busslinger group (The Research Institute of Molecular Pathology, IMP, Vienna, Austria), the heterozygous Pax8 null mice (Pax8^{ko/+}) from Prof. P. Gruss (Max Planck Institute, Goetting, Germany) and Tg-Cre^{ER} transgenic mice from Prof. G. Schutz (DKFZ, Heidelberg, Germany). Wild type C57BL/6J (B6) and 129/SvPasCtrl (Sv) mice were purchased from Charles River Laboratories.

Animals were housed in an animal house under controlled conditions of temperature (22±1°C), humidity (55±10%) and lighting on a 12-h light/12-h dark cycle and were supplied with standard rodent food and water *ad libitum*.

3.3 ES cells screening

ES cells were screened both by polymerase chain reaction (PCR) and Southern blotting.

Both analysis were performed on the genomic DNA isolated from Es cell clones in 96-well plates by an over night incubation at 60°C with 50 µL of lysis buffer (10 mM Tris pH 7.5, 10 mM EDTA pH 8, 10 mM NaCl, 0,5 % sarcosyl with 1.0 mg/ml Proteinase K); the next day 150 µl of cold NaCl/ethanol (75 µM NaCl, in EtOH 100%) is added to each well and incubated for 2 days at 4°C. the DNA pellets are rinsed two-three times with EtOH 70% and resuspended in appropriate volume of distilled water.

PCR screening

I carried out the PCR analysis using the kit “Expand Long Template PCR System” (Roche), according with the manufacturer’s procedure, using the following primers:

F1: 5’-AATCACCTAGAGAAGTCCAC

R1: 5’-CCATGGGGAGGTTGAATGGC

NeoR: 5’-GGGATCGGCCATTGAACAAGATGG

Southern screening

The genomic DNA samples were cut with *ScaI* and the digestion fragments were resolved on a 0.8% (w/v) agarose gel, followed by transfer to a Hybond N⁺ membrane (Amersham Pharmacia Life Science). Hybridization and detection were performed in accordance with the DIG system protocol (Roche). I amplified the probe with the following couple of primers:

SouthF: 5’-TTAGATCTGCTCCATCACATTCGGG

SouthR: 5’-TGTACTAGGCACTCAGCAGGTATGGG

The PCR product was extracted from the gel by “QIAEX II Gel Extraction Kit” (Quiagen), according with manufacturer’s protocol. To DIG-label the probe, I used 10 µg of this product as template for a second PCR performed with the same oligonucleotides with “PCR DIG Probe Synthesis Kit” (Roche).

3.4 Mice screening

All the mice and the embryos described in the present work were genotyped by polymerase chain reaction (PCR) using genomic DNA isolated from the tail clips or yolk sacs.

The tail clips or yolk sacs were incubated over night at 55°C in 700 µL or 500 µL of lysis buffer (50 mM Tris pH 7.5, 100 mM EDTA pH 8, 100 mM NaCl, 1% SDS with 1.0 mg/ml Proteinase K) respectively. The following day genomic DNA was extracted adding 0.3 volumes of 6 M NaCl and precipitated with isopropanol. After washing with 70% ethanol, the DNA pellet was drained at room temperature (RT) and resuspended in appropriate volume of distilled water.

PCR primers

To genotype heterozygous mice for the floxed allele, the PCR was set up so as to identify both the wild type and the recombinant allele using a couple of primers designed at the ends of the loxP inserted in the intron 2 of the gene:

Int2F: 5'-GAAAGTTCGAGGGAAGGGAGATC

Pa1R: 5'-CAGTTCTTTCAGTGGTCCCTCC

These primers amplify a 395 bp product on the recombinant allele and a 300 bp product on the wild type.

To genotype Pax8 heterozygous mice (ko/+), the PCR was set up so as to identify both the wild type and recombinant locus in a single reaction using three different primers: one common forward primer and two reverse primers, one specific for Pax8 wild-type and the other one specific for Pax8 null allele.

The primers used for the amplification were as follows:

wdb: 5'-ATGCTAAGAGAAGGTGGATGAG (in the intron 3)

wrb: 5'-GTTGATGGAGCTGACACTG (in the exon 4)

krb: 5'-TGCACGAGACTAGTGAGAC (in the promoter of the neo cassette).

Primers wdb and wrb amplify a 560 bp product specific for the wt allele; whereas the primers wdb and krb amplify a 455 bp product specific for the mutated allele.

In the case of Pax8^{Cre/+} mice the genotyping was performed as previously described (Bouchard et al 2004).

TgCRE transgene was identified using the following primers:

k7: 5'-AGTCCCTCACATCCTCAGGTT (in the CRE coding sequence)

K8: 5'-ATGCCAACCTCACATTTCTTG (in the CRE coding sequence)

that amplify a 450 bp product specific for CRE.

PCR setup

All PCR reactions were conducted using 100-500 ng of genomic DNA, 1xBuffer (10 mM Tris-HCl pH 8.3, 50 mM KCl, 1.5 mM MgCl₂) 2 μM of common primer, 1 μM of each specific primer, 200 μM of each dNTP, and 0.5 units of Taq polymerase in a final volume of 25 μL. Reactions were performed with the following cycling parameters: 35 cycles of 95°C for 1 min, 58°C for 1 min and 72°C for 1 min.

The PCR products were analyzed by agarose gel electrophoresis.

Agarose gel electrophoresis

The PCR products were analyzed by agarose gel electrophoresis. The agarose gels were cast by melting the agarose in TAE buffer (40 mM Tris-Acetate pH 7.5, 1 mM EDTA) with the addition of the fluorescent dye ethidium bromide to

a final concentration of 0.5 µg/ml. The percentage of agarose in gels was determined depending on the size of DNA fragments to be resolved. Gels were generally run at 90V in 1" TAE buffer and DNA bands were visualized on UV transilluminator.

3.5 Histology, immuno-histochemistry and immuno-fluorescences

Mouse embryos at specific developmental stages were obtained from pregnant females, which were sacrificed by cervical dislocation. Thyroid glands were dissected from embryos or adult mice. Thyroids and embryos were fixed overnight at 4°C in 4% paraformaldehyde (PFA) in phosphate-buffered saline (PBS), pH 7.2, dehydrated through higher grades of alcohol, cleared in xylene, embedded in paraffin blocks and 7µm sections were cut. For histological examinations, serial paraffin sections from DHTP and wild type mice were stained with Harris hematoxylin and aqueous eosin (BDH Laboratory Supplies) or with periodic acid-Schiff reagent-PAS (Sigma) according to the standard protocols.

For immunohistochemical and immunofluorescences studies, paraffin sections of embryos and thyroids were dewaxed in xylene, hydrated through decreasing ethanol grades, washed twice in PBS and once in PBS, 0.2% Triton. To inhibit the endogenous peroxidases, the sections were treated with 0.5% H₂O₂ in absolute methanol for 15 min at RT. Unmasking of the antigen sites was necessary by performing heat treatment of the sections in citrate buffer (0.01 M, pH 6.0). After washes in PBS, the sections were incubated in a humid chamber with histoblock solution (3%BSA, 5% NGS, 20 mM, MgCl₂, 0.3% Tween 20 in PBS, pH 7.2) for one hour at RT to prevent nonspecific staining and further incubation with the primary antibodies was carried out over night at 4°C.

The follow rabbit polyclonal primary antibodies were used:

- anti-Pax8 0,87µg/mL
- anti-Titf1 0,6 µg/mL
- anti-Nis 1:2000 (Dako)
- anti-Tg 0.096 µg/mL
- anti-Calcitonin 1:2000 (Dako)
- anti-Ki67 1:800 (Epicomics)

The incubation with the secondary antibodies was for 1 hour at RT.

The follow anti-rabbit secondary antibodies were used:

- biotinylated anti-rabbit IgC 1:200 (Vector) for the immunihistochemistry
- fluorescein anti-rabbit IgC (Vector) for the Immunofluorescences.

In the immuno-histochemistry, the immunoperoxidase system of the "Vectastain ABC kit" (Vector) was used, and the detection was performed using the "DAB substrate kit for peroxidise" (Vector), according with the manufacturer's protocol. The reaction was controlled under microscope and

stopped in tap water, dehydrated in graded alcohols, cleared in xylene and mounted in EUKITT reagent (BDH).

In the Immunofluorescences experiments, the sections were incubated with DRAQ5 1:1000 (for the nuclei staining) and the slides were mounted with a solution glycerol/PBS1x 1:1, containing Hoechst.

3.6 Hormone measurements

Keeping the mice under light anaesthesia, blood samples from their tail veins were collected in eppendorf tubes without the presence of anticoagulant. After coat formation the samples were centrifuged and the recovered sera were kept frozen at -20°C until assayed.

TSH levels were determined by ELISA assay using the “Rat TSH ELISA Kit” (Gentaur), following the manufacturer’s protocol.

3.7 RT-PCR and Quantitative Real-time PCR

Total RNA was extracted from thyroids using the “TRIzol” reagent (Invitrogen), and 1 µg was used as template for the synthesis of the first reverse cDNA strand by using the “QuantiTect Reverse Transcription” kit (Quiagen), according with the manufacturer’s procedures.

RT-PCR

The RT-PCR performed to screen the Cre-mediated recombinant Pax8 transcript was carried out using 50 ng of cDNA and the following primers:

RTf1: 5’- GCCTCACAACCTCGATCAGATCC

RTr1: 5’- TCAGTGTGTGTCCTGGGCTCA

Real-time PCR

I calculated preliminarily, the amplification efficiency of each primer pairs using cDNA standard dilution series as reported (Rutledge and Cote 2003). RT-PCR amplifications were conducted using 12,5µl of Power SYBR Green PCR master mix (Applied Biosystem), 0.3 µM of each primers a final volume of 25µl. Thermocycling was performed using ABI Prism 7900 Real Time PCR System (Applied Biosystems Foster City, USA). Ct (threshold cycle) values were determined by Applied Biosystems software and analyzed using MS Excel program. For each primer-pair, I generated a standard curve plotting the resulting Ct values against corresponding cDNA dilution series. The slope of the curve was used to calculate the amplification efficiency.

Reactions for quantification of mRNAs were performed in the same conditions as described above, using 20ng of cDNA as a template. The expression of the gene of interest is normalized for the expression of Abelson gene measured under the same condition considering the amplification efficiency of each primer pairs. For each genotype, the data obtained, express as arbitrary units, represent the mean of three independent samples.

The couples of primers used to quantify the several genes analyzed are the following:

Pax8Fw1: 5'-GCCATGGCTGTGTAAGCAAGA (EX3)
 Pax8Rev1: 5'-GCTTGGAGCCCCCTATCACT (EX4)
 Pax8Fw2/5: 5'-CAGTGTCTCAGCTCCATCAACAGAAT (EX2/5)
 Pax8Fw: 5'-AGTGCAGCAGCCATTCAAC (EX5)
 Pax8Rev6: 5'-CTGGGGGTGTTACAGCTGAG (EX6)

Titf1Fw: 5'-CTACTGCAACGGCAACCTG
 Titf1Rev: 5'-CCCATGCCATCATATATTCAT

TgFw: 5'-CATGGAATCTAATGCCAAGAAGCTG
 TgRev: 5'-TCCCTGTGAGCTTTTGGGAATG

TpoFw: 5'-CAAAGGCTGGAACCCTAATTTCT
 TpoRev: 5'-AACTTGAATGAGGTGCCTTGCA

NisFw: 5'-TCCACAGGAATCATCTGCACC
 NisRev: 5'-CCACGGCCTTCATACCACC

AblFw: 5'-TCGGACGTGTGGGCATTT
 AblRev: 5'-CGCATGAGCTCGTAGACCTTC

BclFw: 5'-AGTACCTGAACCGGCATCTG
 BclRev: 5'-CATGCTGGGGCCATATAGTT

TshFw: 5'-TCCCTGAAAACGCATTCCA
 Tshrev: 5'-GCATCCAGCTTTGTTCCATTG

3.8 Array hybridization and data analysis

The embryonic thyroid glands were dissected 1-d-old mice and three samples were pooled for each genotype. Total RNA was extracted with TRIzol. 100 ng of total RNA was processed to generate cRNA by using the Affymetrix One-Cycle Target Labeling and Control Reagent kit (Affymetrix Inc., Santa Clara, California, USA), following the manufacturer's protocol.

The biotinylated cRNA was fragmented and hybridized to the MOGENE 1-0-ST-V1 Affymetrix DNA chips, containing 28815 probesets. Chips were hybridized at 42°C for 16 hours in rotation to ensure mixing, washed and exposed to R-phycoerythrin conjugated streptavidin to evidentiate hybridized biotinylated cRNA. Then they were scanned on the Affymetrix Complete GeneChip Instrument System at a 3µm resolution, generating digitalized image data (DAT) files. The reactions were carried out in triplicate.

DAT files were analyzed with AGCC (Affymetrix, Santa Clara, CA) producing CEL files. RMA normalization and data analysis was performed using GeneSpring 10.1 (Agilent Technologies, Santa Clara, CA).

We consider for the further analysis a probeset if it's expression overcome the 20th percentile in the whole chip distribution in at least 2 of the 3 replicates and in 1 of the 2 conditions. Under this conditions only 25056 probesets are used in the further analysis.

Differentially expressed (DE) genes between Pax8^{Cre/fl} and Pax8^{Cre/+} thyroids were selected on the basis the fold change (the ratio between the expression levels in the two samples) and on the T-test, using as *p-value* a cut off of 0.05.

3.9 Administration of Tamoxifen

Tamoxifen (Sigma) was dissolved in a sunflower oil/ethanol (9:1) mixture at 10mg/mL. In mice at 4 weeks, 50mg/kg tamoxifen were injected every 12 hours for 5 days. One week to three months depending on the experiments, mice were sacrificed and their thyroid dissected.

4. RESULTS AND DISCUSSION

4.1 Generation of a conditional allele of the Pax8 gene

To generate a Pax8 conditional knock-out mouse strain, a targeting vector containing two loxP sites in the same orientation was constructed. The figure 13 shows a schematic representation of the wild-type Pax8 allele, of the targeting vector used to modify it and the Pax8 allele after homologous recombination, together with the corresponding flipped and deleted products. In the targeting vector the positions of the two loxP sites and of the neomycin-resistant cassette are reported. The first loxP site was inserted in the intron 2 of the Pax8 gene, and the second loxP, together with the neomycin-resistant cassette flanked by an FRT site at each end, was inserted in the intron 4; in this way, after a Cre-mediated recombination, we have the depletion of the exons 3 and 4, that codify for the DNA binding domain, with consequent synthesis of a non-functional protein.

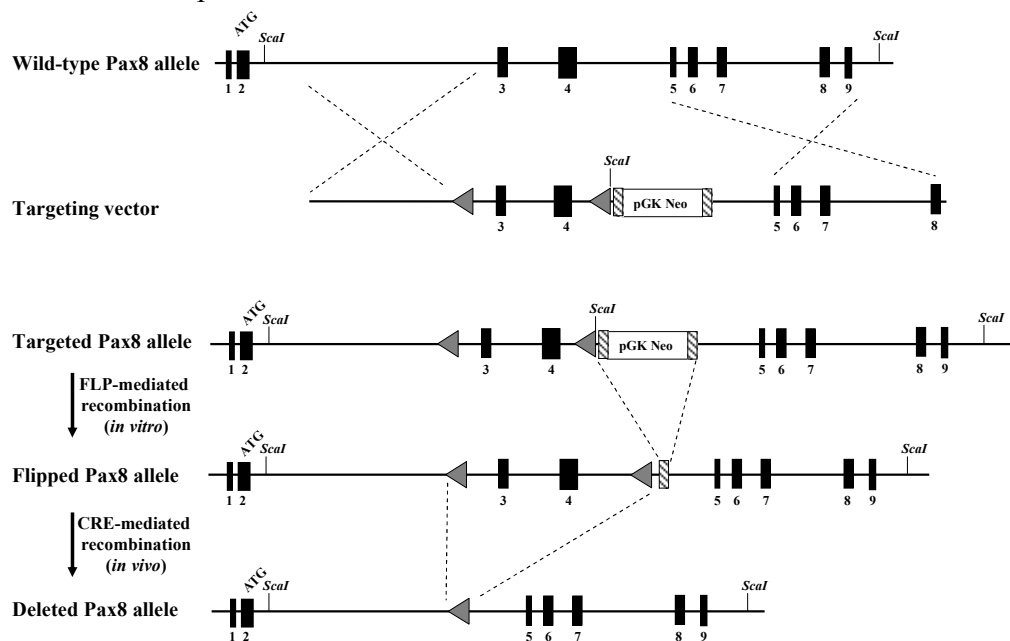


Figure 13 Generation of the Pax8-floxed mouse. Diagram of the Pax8 gene (wild-type allele), targeting vector, targeted allele, flipped allele and deleted allele. The flipped allele is the product of the FLP-mediated recombination between the FRT sites in the ES cells; the deleted Pax8 allele is the product of the Cre-mediated recombination between the loxP sites in mice. The coding regions of the gene are indicated by *solid boxes*. The neomycin cassette is represented by an *open box* marked with pGK-Neo. The loxP and FRT sites are shown by *solid triangles* and *shadow boxes*, respectively. The ATG and the restriction enzyme used for the Southern strategy are indicated.

To generate the construct, I used the recombineering method (also known as Red/ET recombination), a technique that allows for the insertion, deletion, or mutation of DNA sequences, assuaging the need for conveniently located restriction sites.

The process of generating the Pax8 conditional knock-out targeting vector consisted of three main steps (as described in Material and methods):

- 4) retrieval of genomic region of interest from a bacterial artificial chromosome (BAC) onto targeting vector backbone by gap repair;
- 5) insertion of an orphan loxP site;
- 6) insertion of FRT-Neo-FRT-loxP cassette with the same orientation of the orphan loxP site.

The targeting vector DNA was linearized and electroporated in R1 ES cells. To select the clones in which the construct was incorporated in the genomic DNA, the cells were grown in presence of the G418 antibiotic. 300 ES clones were picked and expanded, and their DNA was extracted and analyzed by polymerase chain reaction (PCR).

In figure 14a a schematic representation of the wild-type and targeted Pax8 alleles is shown, with the primers used for the PCR screening indicated with red arrows. In order to discriminate the homologous recombinant clones from the non recombinant ones, the primers (F1/R1 in the scheme) amplify the genomic region going from the intron 2 to the exon 5. Using this strategy, I obtained two different products, a 7500 bps band corresponding to the amplification of the wild type (wt) allele, and a 9500 bps band corresponding to the amplification of the recombinant allele,

Figure 14b shows the result obtained in the screening of the ES clones; 11 out of 300 ES cells screened turned out to be homologous recombinants.

To further validate the results obtained with the first screening, another PCR was performed using the oligonucleotides NeoR and F1 (see Fig. 14c) confirming the genotype of the positive clones.

Finally, in order to check if any undesired random integration event occurred in the selected clones, I performed a Southern blotting; as shown in figure 14d, both wild-type and the recombinant bands are present in the targeted ES clone, while the wild type control only shows the 18600 bp band.

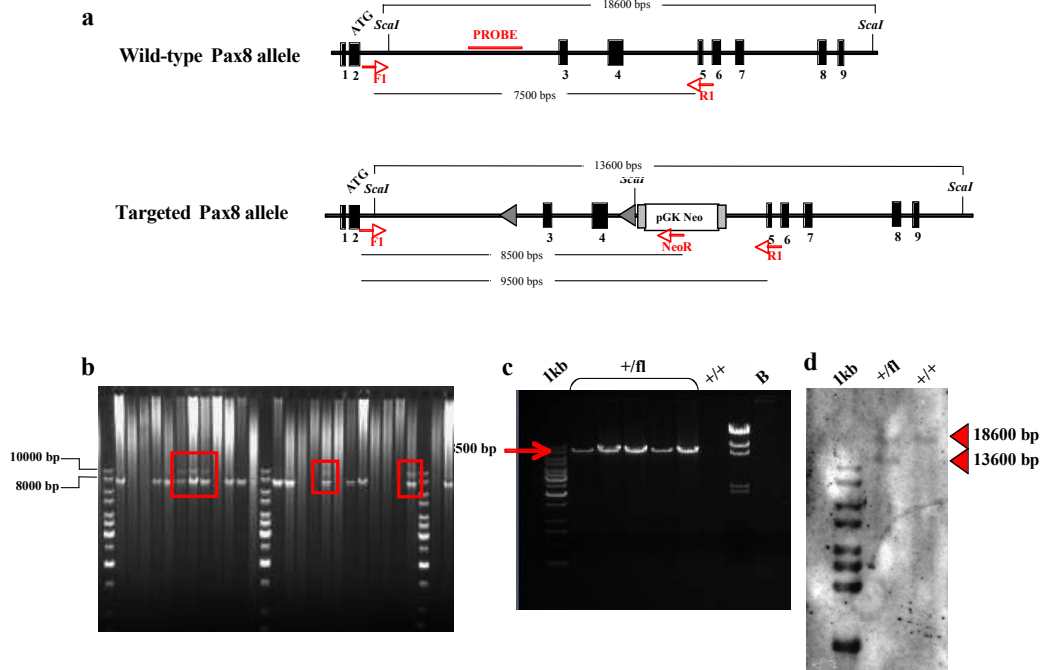


Figure 14 Screening of recombinant ES cells. (a) Diagram of the Pax8 wild-type and targeted allele, the primers used for the screening are indicated; (b) PCR analysis of the ES cells performed with the couple of primers F1/R1 (expected bands: 7500bp wt allele, 9500bp recombinant allele), the positive clones are in the red frame; (c) PCR analysis of the ES cells performed with the F1/NeoR (expected band: 8500bp); (d) Southern blotting analysis (expected bands: 13600bp recombinant allele, 18600bp wt allele). *Solid boxes* indicate the coding regions of the gene. An *open box* marked with pGK-Neo represents the neomycin cassette. The loxP and FRT sites are shown by *solid triangles* and *shadow boxes*, respectively. The primers used for the PCR screenings and the Southern probe are indicated by *red arrows* and *red thin line*, respectively. The ATG and the restriction enzyme used for the Southern strategy are indicated.

To remove the neomycin-resistance cassette, one of the clones was transfected with an FLP-expressing plasmid (see Materials and Methods). 24 clones were picked and grown in absence of the G418. Then DNA was extracted and the FLP-mediated site-specific recombinants were screened by PCR.

In figure 15a a diagram of the wild type, targeted and flipped Pax8 allele are reported: the primers used for the flipped clones screening (F3/R3) are annotated as red arrows. Using these primers, I amplified a 150 bp band on the wild-type allele, a 260 bp fragment on the site-specific recombinant allele and a 2100 bps band on the non-recombinant allele. The panel in figure 15b shows the PCR results. By this screening, I found that 80% of the picked clones were positive for the FLP-mediated recombination.

One flipped ES clone was injected into a C57BL/6 blastocyst, from this injection three chimeric male were born with a chimerism degree higher than 70% and they were bred with C57BL/6 females to generate heterozygous loxP targeted/wild-type mice (Pax8^{fl/+}). These mice were screened by PCR using a couple of primer (Int2F/Pa1R in figure 15a) designed at the ends of the insertion point of the orphan loxP. With this strategy I obtain a 300 bp band, that identifies the wt allele, and a 395 bp band, resulting from amplification of the floxed allele, longer than the wt band because of the loxP site insertion.

The picture 15c represents the analysis carried out on DNA extracted from tail-biopsies. Pax8^{fl/+} mice are viable and healthy and follow the expected mendelian ratio.

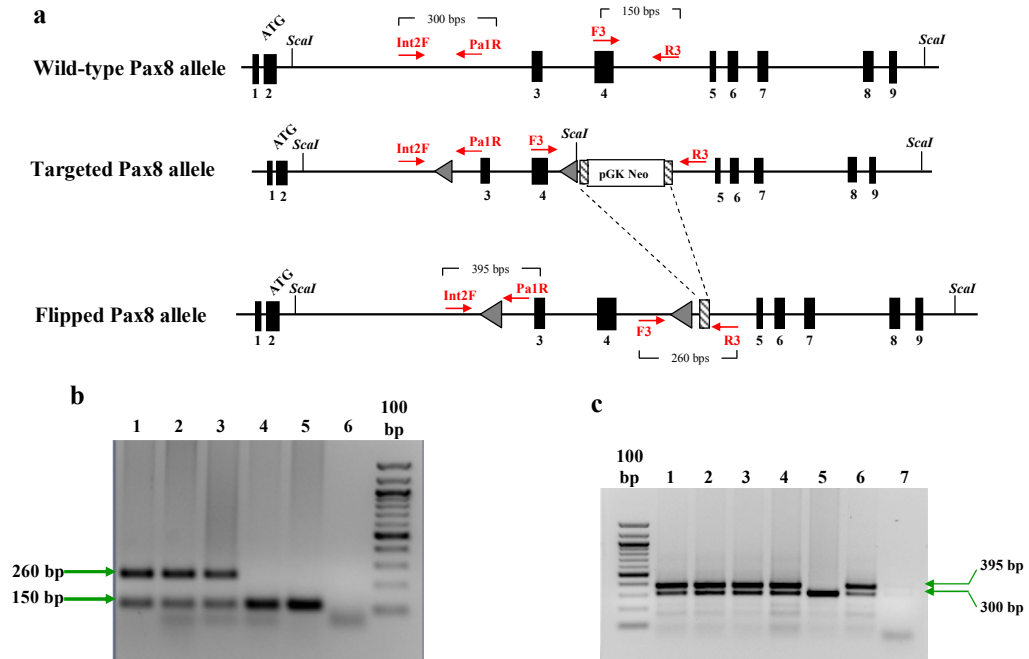


Figure 15 Screening of flipped ES clones and germ line transmission. (a) Diagram of the Pax8 wild type, targeted and flipped allele, the primers used for the screening PCR are indicated as *red arrows*; (b) PCR analysis on the Flp-mediated recombinant clones to remove the neomycin-resistant cassette (expected bands: 260 bp flipped allele, 150 bp wt allele), lanes 1-3 recombinant clones, lane 4-5 wild-type DNA, lane 6 blank; (c) PCR analysis on tail-extracted DNA of mice born from chimera crossed with females C57BL/6 (expected bands: 395 bp floxed allele, 300 bp wt allele), lane 1-4 heterozygous mice Pax8^{fl/+}, lane 5 wt DNA, lane 6 ES positive clone DNA, lane 7 blank. *Solid boxes* indicate the coding regions of the gene. An *open box* marked with pGK-Neo represents the neomycin cassette. The loxP and FRT sites are shown by *solid triangles* and *shadow boxes*, respectively. The length of the PCR products is indicated with *green arrows*.

4.2 Cre-mediated recombination of floxed Pax8 allele: deletion of the floxed Pax8 allele mediated by Pax8-Cre (strain Pax8^{Cre/fl})

To selectively drive the deletion of the Pax8 allele in the thyroid gland, heterozygous mice for the floxed Pax8 allele (Pax8^{fl/+}) were bred with the Pax8^{Cre/+} knock-in mice (Bouchard et al. 2004), described in the paragraph 1.4.1. This breeding scheme generated mice with the following genotypes: Pax8^{+/+}, Pax8^{+/-Cre}, Pax8^{+/-fl} and Pax8^{Cre/fl} (Fig. 16).

Since the Cre-driver strain used for these experiments is a knock-in with the recombinase inserted in the Pax8 endogenous locus, one recombination event *per cell* is sufficient to completely delete every Pax8 function.

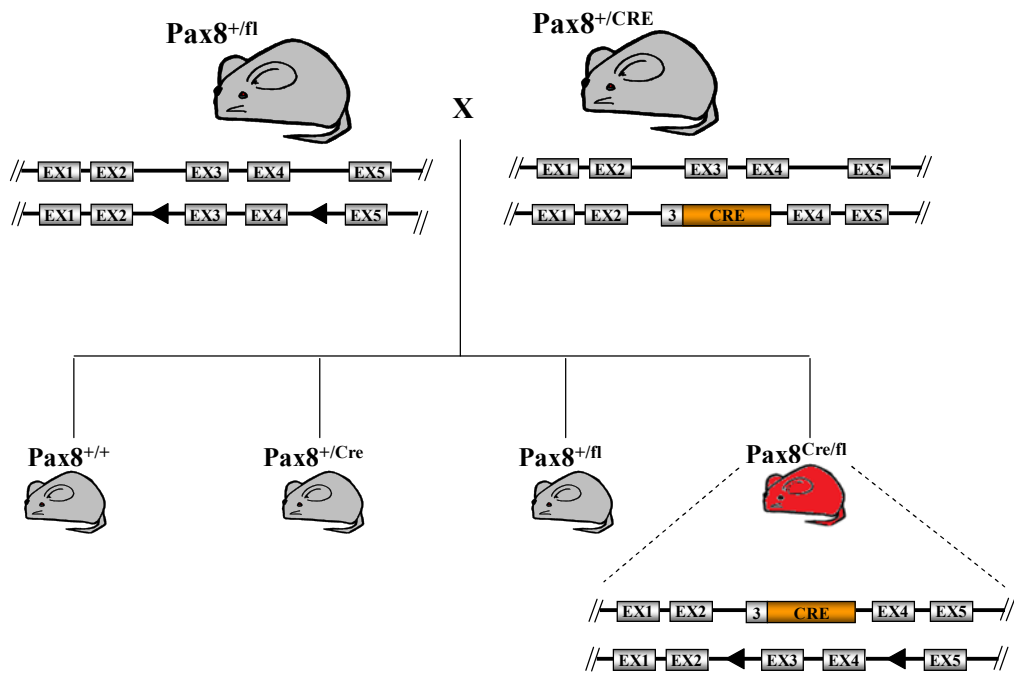


Figure 16 Breeding scheme between the heterozygous mice for the floxed Pax8 allele and the heterozygous mice for the Pax8-Cre allele. The coding regions are represented by boxes, grey for Pax8 and orange for Cre; the exons are numerated. The solid triangles indicate the loxP sites.

To confirm that Cre-mediated recombination occurred in the floxed Pax8 allele *in vivo*, a result of exons 3 and 4 deletion, a RT-PCR (see MATERIALS AND METHODS) was carried out using thyroids obtained from embryos at embryonic day (E) 16.5 and 17.5. As illustrated in the scheme of the figure 17a, for this experiment a couple of primers was designed to amplify the transcript region extending between the exons 2 and 5, in order to generate two different PCR products: a shorter band on the recombinant transcript and a longer fragment on the wild type.

In figure 17b and c it is represented a correct recombination between the two loxP sites: as shown by RT-PCR results, the 476 bp band (wt band) is still present at E16.5, indicating that the recombination is not complete, while at E17.5 the wild type band becomes very faint.

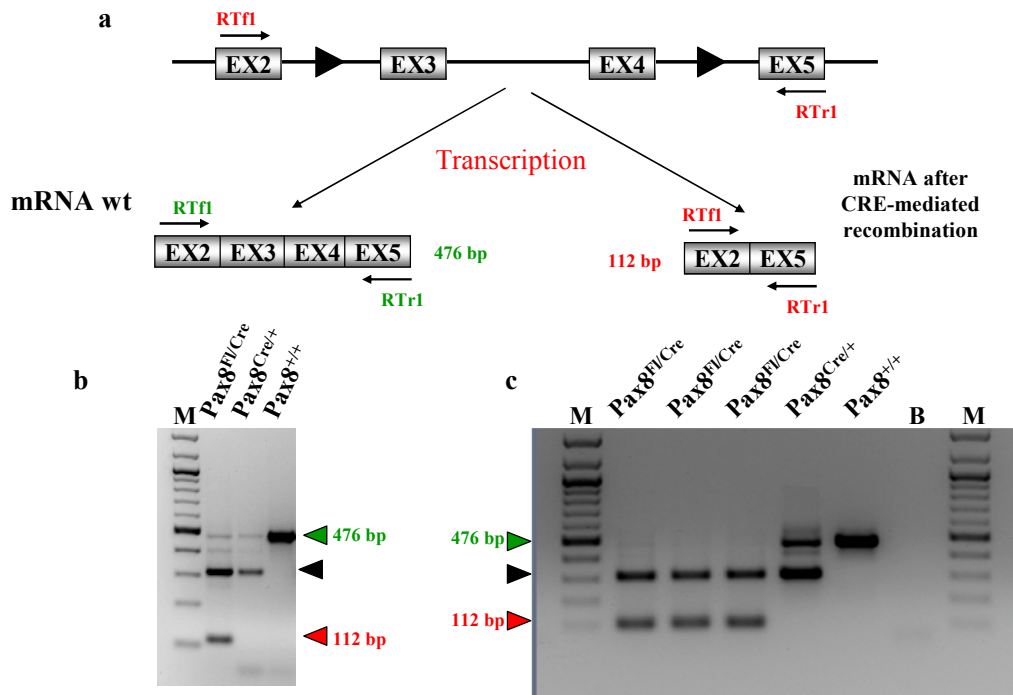


Figure 17 Cre-mediated recombination in embryonic thyroids. (a) The primer RTfl recognizes the exon 2 and the primer RTr1 the exon 5; the expected bands were of 476 bps on the wt transcript and 112 bps on the recombinant one. The coding regions are represented by *grey boxes*, loxP sites by *solid triangles*; (b) RT-PCR performed on thyroids collected from embryo E16.5; (c) RT-PCR performed on thyroids collected from embryo E17.5. *Green* and *red arrowheads*, indicate wt and recombinant products, respectively. The 300bp band, black arrowhead, is a non-specific product in the PCR reaction due to the presence of the Pax8-Cre allele.

4.2.1 Thyroid morphogenesis in Pax8^{Cre/fl} mice

Since Pax8 is expressed by E8.5, I decided to analyze thyroid development in Pax8^{Cre/fl} mice. Embryos at the stages of E12.5 and E14.5, obtained from crosses of Pax8^{fl/+} with Pax8^{Cre/+} mice, were collected and analyzed.

The panel in figure 18 shows hematoxylin-eosin staining of histological sections from Pax8^{Cre/fl}, Pax8^{Cre/+} and Pax8^{+/+} embryos at the stage of E12.5 and E14.5. At both stages, the histological analysis reveals that developing thyroid is comparable in size and shape in all the genotypes.

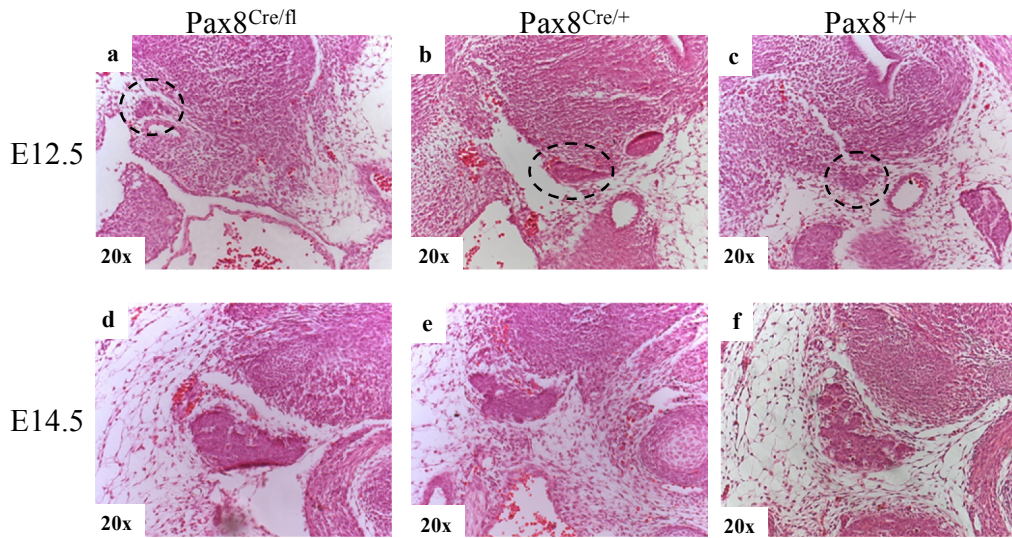


Figure 18 Hematoxylin and Eosin staining on sagittal paraffin-embedded sections of E12.5 and E14.5 embryos. (a-c) H&E staining on E12.5 Pax8^{Cre/fl}, Pax8^{Cre/+} and Pax8^{+/+} embryos, respectively. The developing thyroid is indicated with a *dashed circle*; (d-f) H&E staining on E14.5 Pax8^{Cre/fl}, Pax8^{Cre/+} and Pax8^{+/+} embryos, respectively. The size of the developing thyroid in Pax8^{Cre/fl} embryos is not different from that of the control embryos.

Afterwards, we analyzed the expression of thyroid-specific markers, such as *Titf1* and Thyroglobulin (Tg), that starts to be detectable at the embryonic stage of 14.5. As figure 19 shows, both proteins were comparably expressed in the Pax8^{Cre/fl} developing thyroid and the controls.

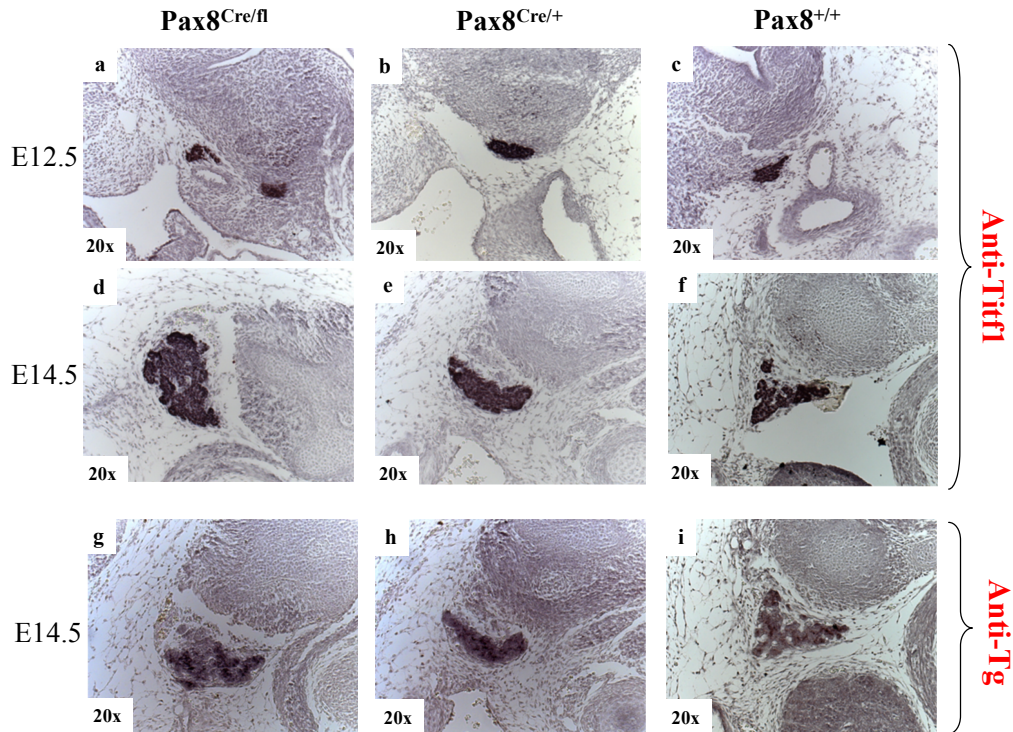


Figure 19 *Titf1* and *Tg* immunostaining on sagittal paraffin-embedded sections of E12.5 and E14.5 embryos. The antibodies used and the embryonic stage and the genotype of the samples analyzed are indicated. Both *Titf1* (a-f) and *Tg* (g-i) expression are unaltered in the two samples.

All together, these data suggest that during embryonic development the Cre-mediated deletion of the floxed allele could not be sufficient to impair thyroid morphogenesis. To determine whether *Pax8* was still expressed in developing thyroid, I performed an immuno-histochemistry on embryo sections at the stage of E12.5 and E14.5: as shown in figure 20, *Pax8* levels appears not to be affected. Hence, the lack of the phenotype is due to an inefficient deletion of *Pax8*.

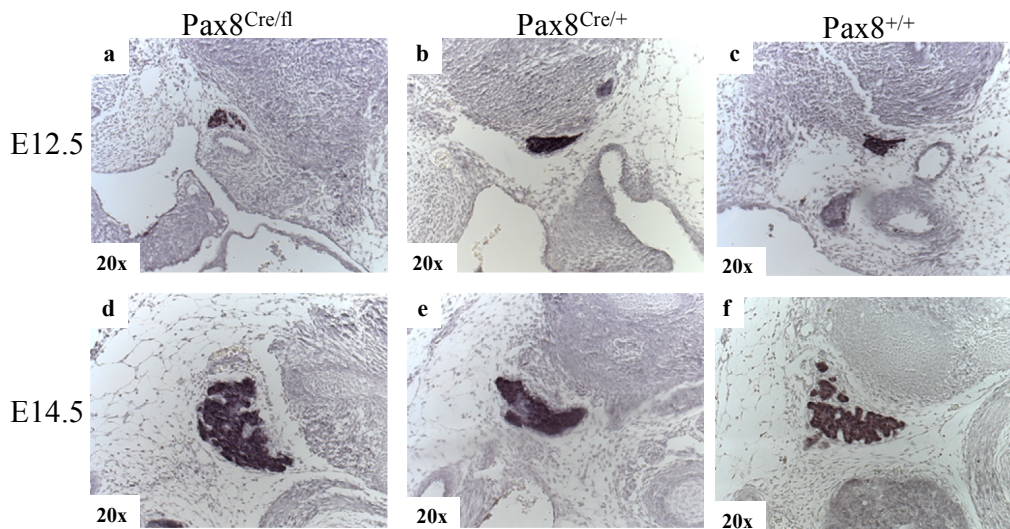


Figure 20 Pax8 immunostaining on sagittal paraffin-embedded sections of E12.5 and E14.5 embryos. The embryonic stage and the genotype of the samples analyzed are indicated. Pax8^{Cre/fl} embryos did not show differences in Pax8 expression.

From this analysis we can conclude that, despite the recombinase in the Pax8-Cre mice starts to be expressed at the embryonic stage of 8.5, its expression levels are probably not sufficient to mediate the recombination in the majority of the thyrocytes during gland organogenesis. These data are consistent with the finding that Pax8 Cre-mediated recombination in developing kidney appears to be discontinuous and inefficient, particularly in heterozygous Pax8^{Cre/+} mice (Bouchard et al 2004)

4.2.2 Analysis of the structure and function of the thyroid in Pax8^{Cre/fl} mice

To check whether Cre-mediated recombination between the loxP sites was complete in the 1-month-old Pax8^{Cre/fl} mice, I performed RT-PCR, as previously described in paragraph 4.2 (Fig. 21). This analysis showed that in the mutant samples the wild-type band has completely disappeared (476 bp).

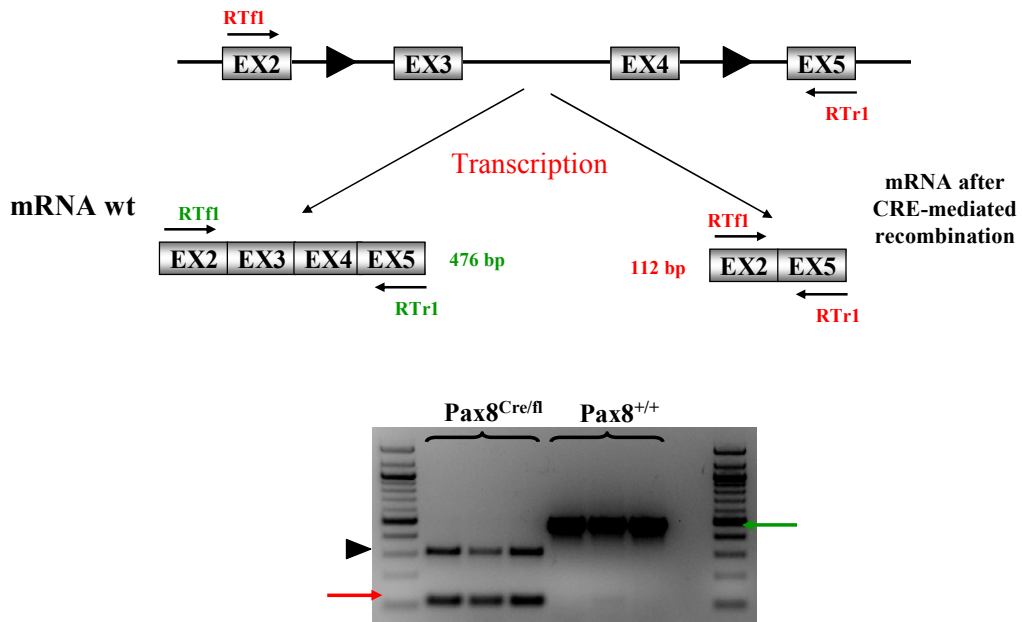


Figure 21 Cre-mediated recombination in 1-month-old thyroids. (a) The primer RTfl recognizes the exon 2 and the primer RTr1 the exon 5; the expected bands were of 476 bps on the wt transcript and 112 bps on the recombinant one; (b) RT-PCR performed on thyroids collected from 1-month-old mice. The wild-type band is completely disappeared in the Pax8Cre/fl cDNAs. The coding regions are represented by *grey boxes*, loxP sites by *solid triangles*. *Green and red arrows* indicate wt and recombinant products, respectively. The 300bp band, black arrowhead, is a non-specific product in the PCR reaction due to the presence of the Pax8-Cre allele.

To confirm that the expression of Pax8 was down-regulated, I carried out a real-time PCR (see Materials and Methods). The couple of primers used for this experiment were designed at the exons 3/4 junction, to selectively amplify only the non-recombinant allele. I performed this experiment on pools of RNA extracted from the thyroid of three different 1-month-old mice for each genotype, and the results are represented in the graph of the figure 22. This analysis revealed that in the Pax8^{Cre/fl} mice Pax8 transcript is strongly reduced compared both to the wild-type and the heterozygous for the Pax8-Cre allele mice.

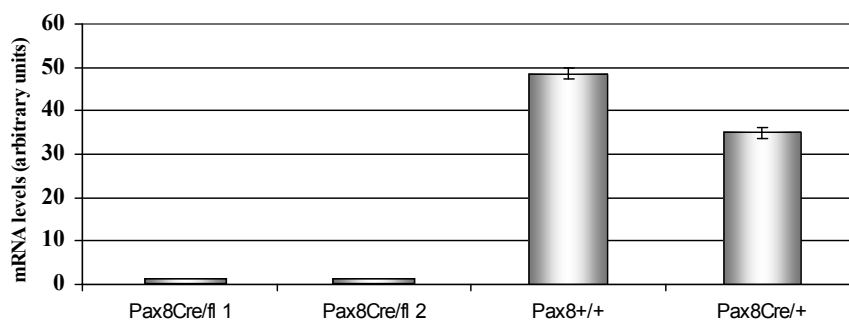


Figure 22 Real-time PCR performed to quantify the wild-type Pax8 transcript. The cDNAs used for this experiment were retro-transcribed from pools of RNAs extracted from the thyroids of 5 1-month-old mice for each genotype. Two different Pax8^{Cre/fl} pools were used and in both sample the Pax8 expression

is almost undetectable. The Pax8^{Cre/+} mice are characterized by reduced Pax8 levels respects to the wild type since they have only a copy of the gene.

Thyroid function

Mice born from crosses of Pax8^{fl/+} and Pax8^{Cre/+} lines respects the mendelian ratio.

One month after birth, Pax8^{Cre/fl} mice appear smaller then their littermates (Fig. 2a). A comparison of body weight of these mice showed that there are statistically significant differences between the conditional knock out and the wild-type mice (Fig. 23 b, c), while Pax8^{Cre/+}, Pax8^{fl/+}, Pax8^{+/+} body weights are comparable.

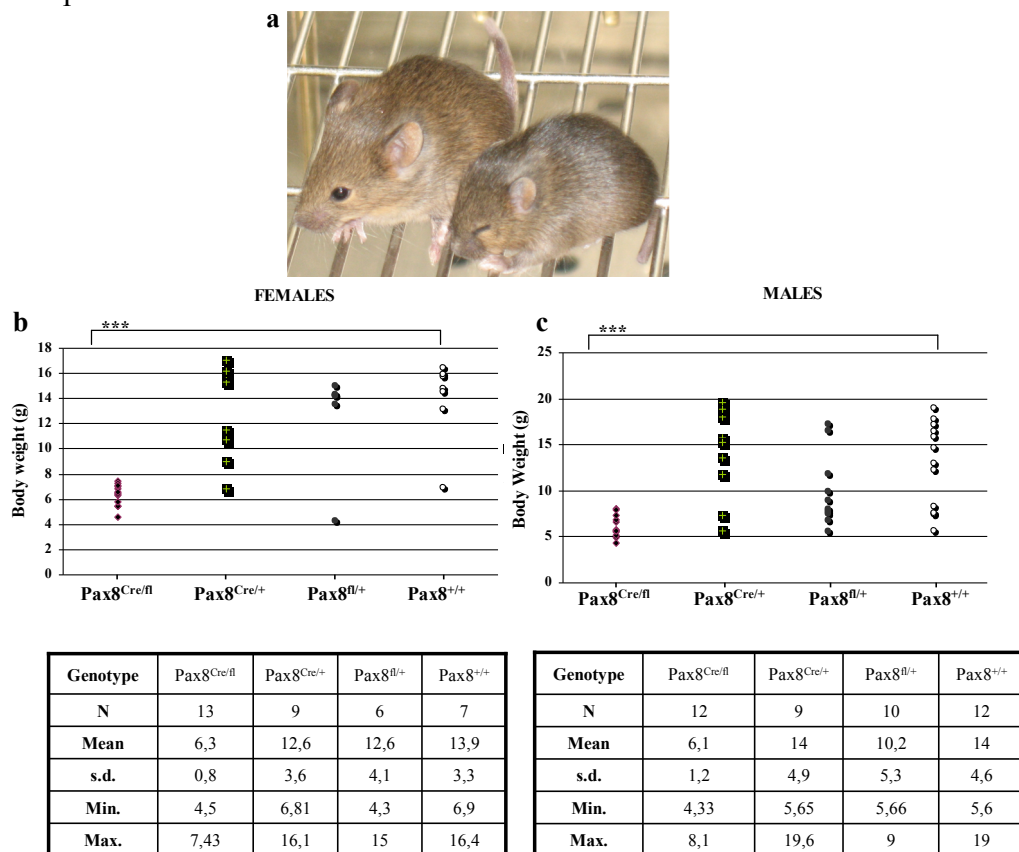


Figure 23 Body weight graphs of the 1-month-old mice born from crosses of Pax8^{fl/+} and Pax8^{Cre/+} lines. (b,c) Each point represents a value for a single mouse.

The tables show mean, s.d, minimum and maximum values for each genotype.

*** = p < 0.001 Pax8^{Cre/fl} versus wt or single heterozygous mice by unpaired, two tailed Student's t test.

Since the adult body weight is a physiological parameter under the control of thyroid hormones, postnatal growth defects can be associated with a deficiency in thyroid gland function.

TSH level is considered to be a critical indicator of the severity of the pituitary-thyroid axis dysfunction (Murray D 1998): thus I decided to investigate the

thyroid functionality by measuring TSH serum levels through an ELISA assay (see Materials and Methods) performed on the blood serum of 5 different 1-month-old mice for each genotype.

The results, reported in figure 24, show that Pax8^{Cre/fl} mice have a mean serum TSH concentration 4-fold higher than the control samples, while the results obtained for the Pax8^{Cre/+}, Pax8^{fl/+}, and Pax8^{+/+} mice are comparable.

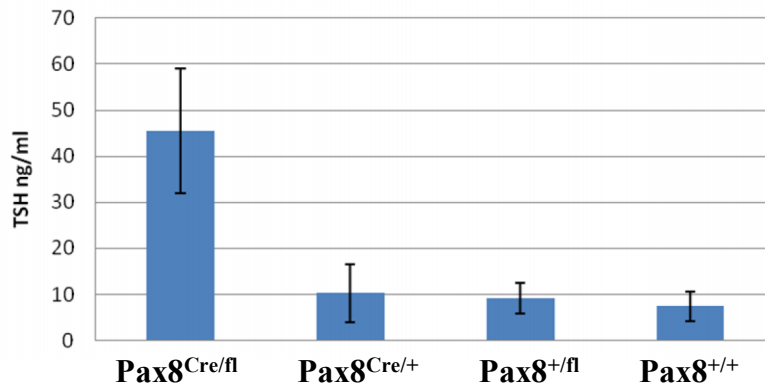


Figure 24 Serum TSH levels in Pax8^{Cre/fl}, Pax8^{Cre/+}, Pax8^{fl/+} and Pax8^{+/+} 1-month-old mice. For each genotype, 5 different samples were analyzed.

Taken together, these findings demonstrate that the Pax8^{Cre/fl} mice are affected by a severe hypothyroidism, since their thyroid is not able to secrete a sufficient amount of hormones.

Thyroid structure

To analyze the structure of the thyroid gland, we dissected the thyroids from 1-month-old Pax8^{Cre/fl}, Pax8^{Cre/+} and Pax8^{+/+} mice.

As figure 25 shows, in Pax8^{Cre/fl} mice the thyroid gland is remarkably smaller compared to control thyroid from either wild-type or Pax8^{Cre/+} mice (panel 25 a-c). Moreover, histological analysis indicates that the follicular structure of Pax8^{Cre/fl} thyroid is strongly impaired and it is not possible to distinguish any follicular structures (panel 25 e-f).

All the experiments performed until this point demonstrate that in Pax8^{Cre/+} mice both thyroid structure and thyroid function are similar to those of wt mice (Fig. 24-25). Furthermore, immuno-histochemistry assays (data not shown) demonstrate that Titf1, Foxe1 and Tg are expressed at comparable levels in both the murine lines.

Hence, from now on, only Pax8^{Cre/fl} mice were compared with Pax8^{Cre/fl} mice.

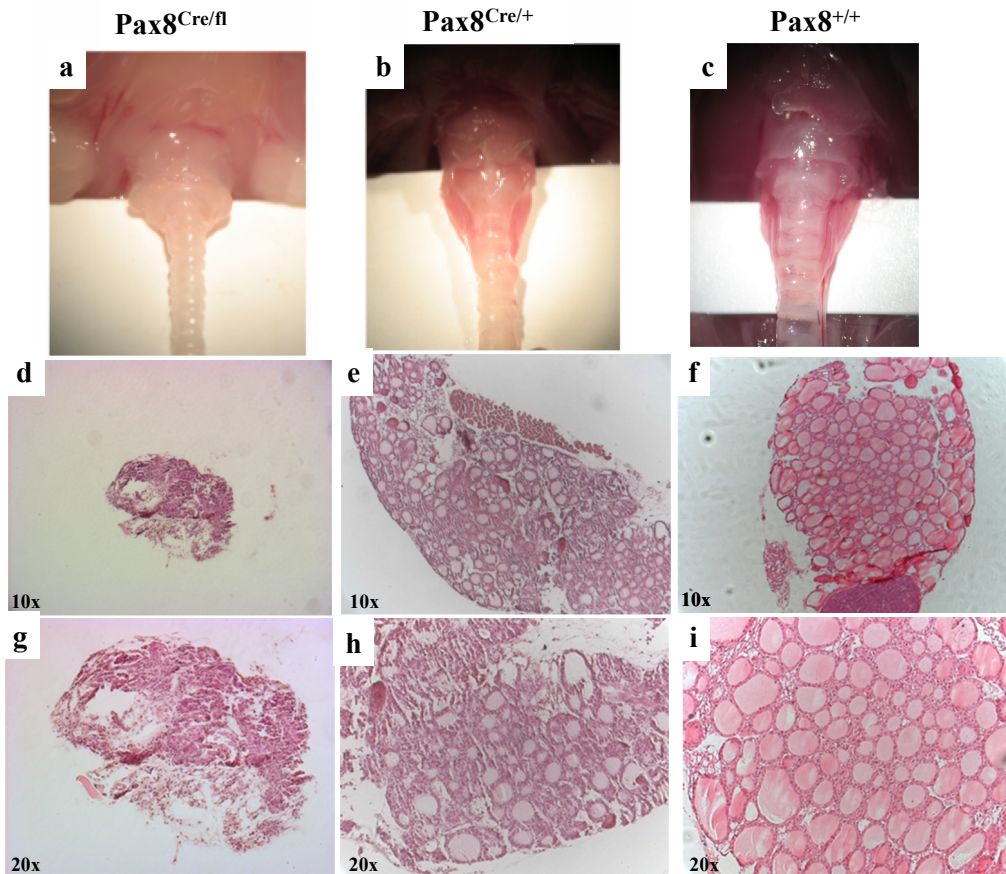


Figure 25 Morphology and histology of 1-month-old thyroids. The Pax8^{Cre/fl} (a) thyroid is smaller than the controls (b-c). (d-i) Hematoxylin-eosin staining of sagittal paraffin-embedded thyroid sections; the Pax8^{Cre/fl} (d,g) sections have lost the follicular structure typical of the normal glands (e,f,h,i).

4.2.3 Molecular phenotype of thyroid in Pax8^{Cre/fl} mice: gene expression analysis

Several genes encoding proteins involved in the thyroid hormone biosynthetic machinery have been proposed to be under the control of Pax8 (Damante et al. 2001). To investigate whether the decreased levels of this transcriptional factor affect the expression of thyroid-enriched genes, such as thyroglobulin (Tg), thyroperoxidase (TPO), TSHR, NIS and Titf1, mRNA levels of these genes were analyzed with a quantitative RT-PCR performed on RNA extracted from 1-month-old Pax8^{Cre/fl} and Pax8^{Cre/+} thyroids.

The panel in figure 26 shows that, compared to the control, the expression levels of Tg, TPO, NIS and TSHR were significantly reduced in Pax8^{Cre/fl}, while Titf1 transcription levels are not significantly affected by Pax8 inactivation.

Furthermore, recent data from our lab (Fagman et al. in press) have confirmed that, *in vivo*, Pax8 regulates the expression of Bcl2, as already reported in cell line (Hewitt et al. 1997). Hence we decide to analyze the expression of Bcl-2 too, whose expression, as shown in figure 26, is reduced in Pax8^{Cre/fl} mice.

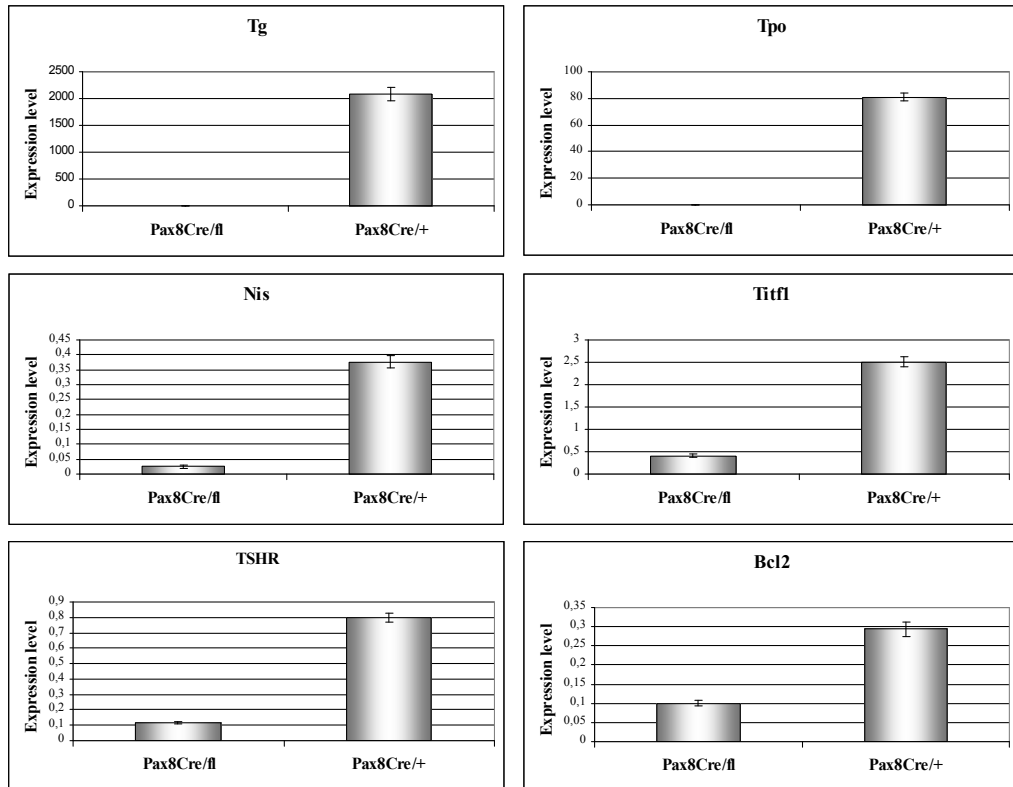


Figure 26 Real-time PCR of thyroid-specific genes in Pax8^{Cre/fl} and control thyroids. For each genotype, the data represent the mean of three independent samples, each representing RNA pooled from three 1-d-old thyroid. The amount of transcript in the samples is expressed in arbitrary units as the ratio between the amount of sample and the amount of Abelson transcript, the endogenous control. In Pax8^{Cre/fl} mice, the expression of Tg, Tpo, Nis, Tshr and Bcl-2 appears significantly affected by the deficiency of Pax8.

To validate the data obtained from the quantitative analysis performed by real-time PCR, an extensive immuno-histochemistry analysis was carried out using serial sections of whole thyroids.

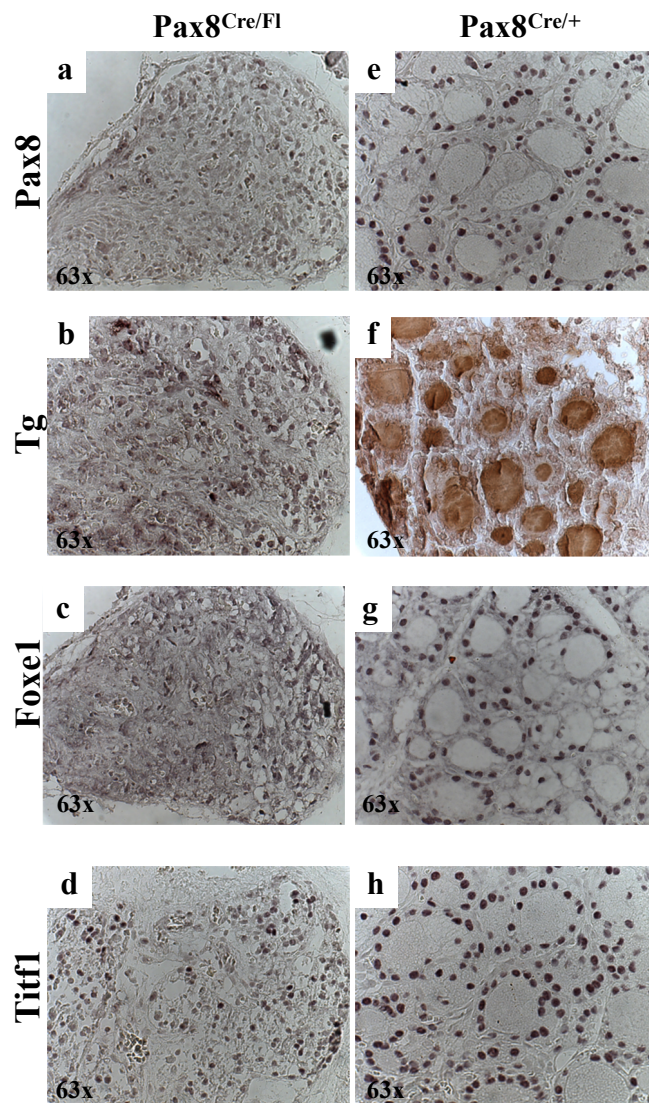


Figure 27 Immunostainings on serial thyroid paraffin-embedded sections of 1-month-old $Pax8^{Cre/Fl}$ and $Pax8^{Cre/+}$ mice. The antibody used and the genotype of the samples analyzed are indicated. In $Pax8^{Cre/Fl}$ thyroids sections (a-d) only the transcription factor Ttf1 is detectable, while the other markers, clearly visible in control samples (e-h), are undetectable.

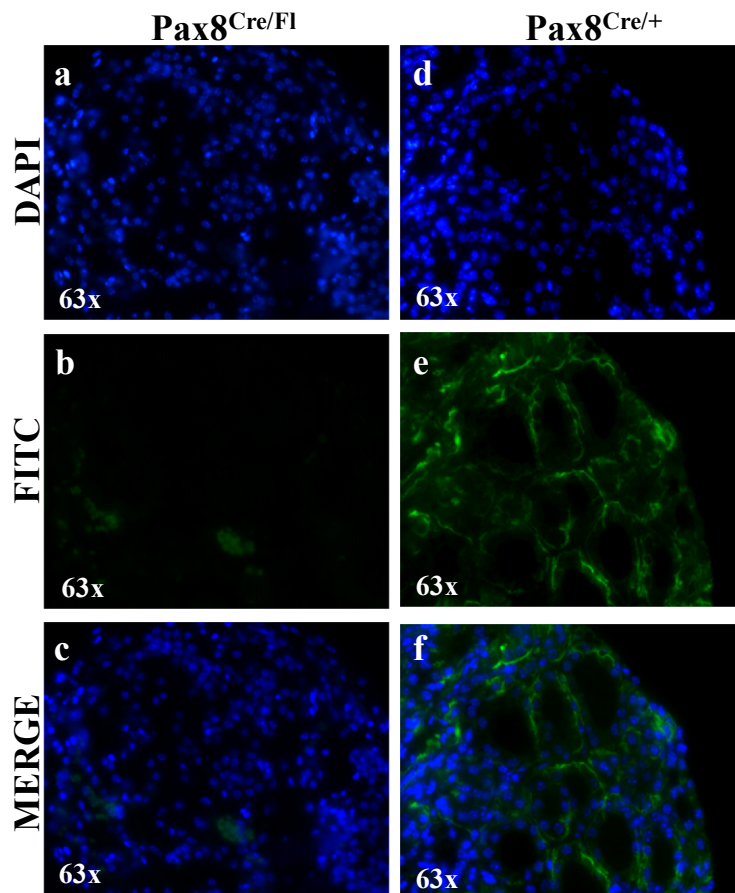


Figure 28 Immunofluorescent staining of Nis in Pax8^{Cre/fl} and Pax8^{Cre/+} DAPI staining was used for the detection of the nuclei. The merge between the two probes is shown. The typical NIS signal is clearly visible on the baso-lateral membrane of the Pax8^{Cre/+} thyrocytes (e,f), while in the Pax8^{Cre/fl} thyroid (b,c) any signal is detectable .

Figures 27 and 28 show 1-month-old Pax8^{Cre/fl} and Pax8^{Cre/+} thyroid sections stained with Pax8, Tg, Foxe1, Titf1 and NIS antibodies. All these proteins seem to be strongly down-regulated (Fig. 27 a,b,c, Fig. 28 b) except for Titf1 (Fig. 27 d) where is still possible to distinguish many nucleus stained for this protein, even if the follicular structure is impaired.

From the results of the real-time PCR and immunostaining experiments we assume that Pax8 is not expressed and many genes usually expressed in thyroid differentiated cells are down-regulated exception made for Titf1 whose expression seems not to be affected.

In thyroid gland, calcitonin-producing cells (C-cells) coexist with thyroid follicular cells and, although different from follicular cells in function and embryological derivation, also express Titf1 (Suzuki et al. 1998). For this reason I wondered if Titf1-positive cells present in Pax8^{Cre/fl} thyroid were follicular cells or calcitonin cells. To answer this question, serial sections of a Pax8^{Cre/fl} thyroid were stained with anti-calcitonin and anti -Titf1 antibodies.

As the figure 29 shows, *Titf1* positive cells are distributed in all the section, but the calcitonin signal is localized only in restricted areas.

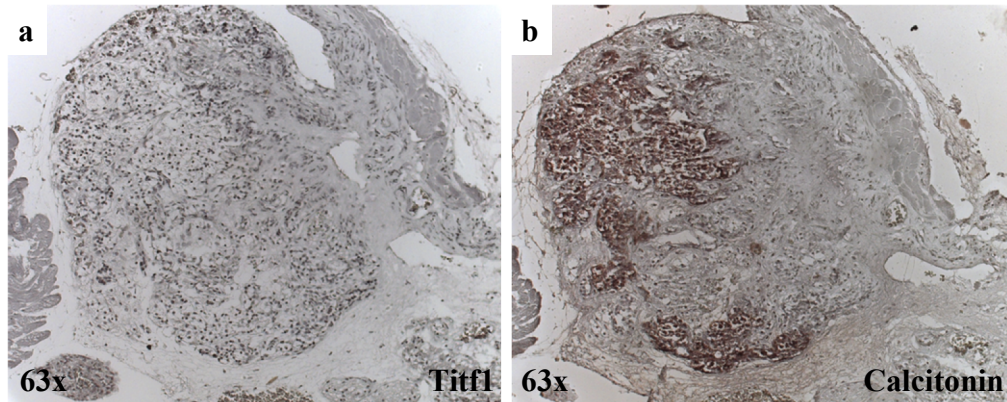


Figure 29 Comparison between *Titf1*- and Calcitonin-stainings of serial paraffin-embedded thyroid sections of *Pax8^{Cre/fl}* 1-month-old mice. (a) *Titf1*-positive nuclei are uniformly distributed on the section, while the calcitonin signal is localized only in restricted area of the thyroid (b). This finding indicates that a large part of *Titf1* positive cells are not C-cell.

These results were confirmed on thyroids isolated from different mice.

Taken together, these findings confirm that *in vivo* Pax8 plays an important role in the maintenance of the thyroid differentiated phenotype, by regulating the expression of genes like TG, TPO, NIS and TSHR, that are essential for the gland physiology (Ohno et al. 2004, Pasca di Magliano et al. 2000, Fabbro et al. 1998), and of *Foxe1*, that was already suggested to be a Pax8 downstream target (Parlato et al. 2004).

4.2.4 Global gene expression profile in *Pax8^{Cre/fl}* thyroid mice

To define the entire spectrum of changes in gene expression related to the inactivation of the Pax8 gene, I decided to analyze the global gene expression profiles in thyroid dissected from *Pax8^{Cre/fl}* and *Pax8^{Cre/+}* mice. Since I was interested to investigate the early effect of Pax8 absence, preliminarily I analyzed the time course of Pax8 down-regulation. To this aim, I collected *Pax8^{Cre/fl}* and *Pax8^{Cre/+}* thyroids at several embryonic stages, E18.5, 1 day and 2 weeks after birth, and I evaluated the total amount of Pax8 transcribed by real time PCR (data not shown). Finding that in 1-d-old mutant mice Pax8 expression was already completely absent. According to this experiment I chose to analyze the global transcriptome in 1-d-old *Pax8^{Cre/fl}* thyroids.

RNAs from *Pax8^{Cre/fl}* and *Pax8^{Cre/+}* were pooled and analyzed, using the Affimetrix mouse expression set MOGENE 1-0-ST-V1 GeneChips covering 28,815 mouse transcripts. For each genotype, three independent RNA samples were used, each representing RNA pooled from three thyroids. Statistically significant differences in the levels of gene expression between conditional

knock-out and control samples were identified with values of $P \leq 0.05$ and fold changes ≥ 1.5 .

25,056 transcripts had a detectable expression in thyroid.

In figure 30 a hierarchical clustering of the differentially regulated genes is shown in two-dimensional matrix.

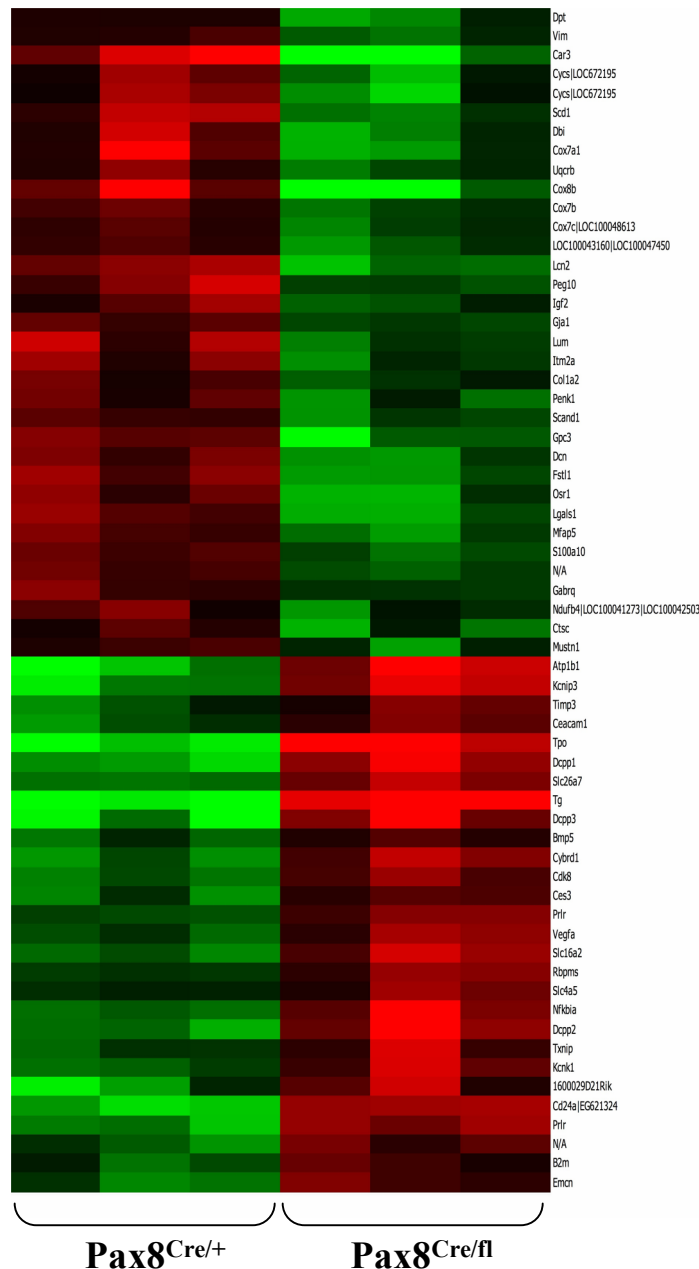


Figure X30 Two dimensional hierarchical clustering. Data from MOGENE 1-0-ST-V1 Affimetrix chips identifying mRNAs significantly regulated in Pax8^{Cre/fl} thyroids in comparison with the control are shown. Intensity in the *red* and *green* range indicates the increase and decrease in mRNA abundance, respectively. Each *row* represents a single gene; each *column* represents a particular experimental sample; each *box* represent a normalized gene expression value.

Considering the high number of transcripts found expressed in the thyroid, only 58 genes appear to be modulated in Pax8^{Cre/fl} compared with Pax8^{Cre/+} of the same age. 39 out of 58 are already known to be expressed in thyroid as reported in tables 1 and 2.

Because of the restricted number of genes, analysis based on either Go Classification or Ingenuity Pathway Analysis (IPA), directed to find their most significant biological functions, did not produce reliable results. So, we decided to characterize the list of genes according to their biological function as reported in the scientific literature.

This rough analysis strongly suggested that these differentially expressed genes are functionally correlated.

Among the up regulated genes, the top seven are implicated, directly or indirectly, in cell death pathway. In particular, Car3 (Carbonic anhydrase) may act as a member of the immune system against oxidative stress (Kim et al. 2004); cytochrome oxidases, (Cox8b and Cox7a1) stimulate caspase activation via cytochrome c oxidation (Borutaite and Brown 2007); Lipocalin-2, which binds or transports lipid and other hydrophobic molecules, is considered a pro-apoptotic protein (Kehrer 2010); GPC3 inhibits the PI3K/Akt anti-apoptotic pathway (Buchanan et al. 2010); Lgals1 (Galectin-1) and Fstl1 are known to promote the apoptosis (Motran et al. 2008, Chan 2009). It is worth noting that the anti-apoptotic gene Bcl2 was down regulated as previously demonstrated by Real Time PCR experiments (see Fig. 26).

Pro-apoptotic genes up-regulation and anti-apoptotic genes down-regulation suggests a shift toward apoptosis which fits with the observed morphological phenotype of the thyroid in Pax8^{Cre/fl} mice.

The most down-regulated genes are Tg and TPO; several studies in cell lines proved that expression of both these genes is regulated by Pax8 (Pasca di Magliano et al. 2000, Fabbro et al. 1998). Another well known Pax8 target, NIS (Ohno et al. 2004), is not included in the present list probably due to its low expression levels; however, data presented in figure 26 and figure 28 clearly indicate that this protein is absent in Pax8^{Cre/fl} mice.

Other down-regulated genes identified have not yet been described as a target of Pax8. Atp1b1 encodes for the beta subunit of Na⁺/K⁺-ATPases localized on the basolateral membranes of thyroid follicular cells; the electrochemical sodium gradient generated by the Na⁺/K⁺-ATPases is required to drive the NIS-mediated transport of iodide. Kcnip3 (DREAM) modulates the transcriptional activity of Titf1 (D'Andrea et al. 2005). CD24, a polypeptide molecule is supposed to play a role in the thyroid regeneration (Chen et al. 2009). Prlr, prolactin receptor, is detected in normal and neoplastic human thyroid tissues as well as in the developing thyroid (Fagman and Di Lauro, personal communication); its role in thyroid is still unknown.

Dcpp1 and Dcpp2 genes encode for demilune cell and parotid protein 1 and 2 respectively; interestingly, Dcpp shows a 70-fold up-regulation in thyroid from transgenic mouse over-expressing the Adenosine Receptor 2a (Goffard et al. 2004).

Table 1 Genes down-regulated in Pax8^{Cre/fl} thyroid versus Pax8^{Cre/+} thyroid

Gene name	Description	Expressed in thyroid*	Fold change
Tg	Thyroglobulin	Yes	7,2
Tpo	Thyroid peroxidase	Yes	5,6
Dcpp3	Demilune cell and parotid protein 3	1,2	3,4
Atp1b1	ATPase, Na ⁺ /K ⁺ transporting, beta 1 polypeptide	Yes	3,3
Dcpp1	Demilune cell and parotid protein 1	1,2	3
Cd24a	CD24a antigen	Yes	3
Dcpp2	Demilune cell and parotid protein 2	1,2	3
Kcnip3	Kv channel interacting protein 3, calsenilin	Yes	2,9
Prlr	Prolactin receptor	Yes	2,4
Nfkbia	Nuclear factor of kappa light polypeptide gene enhancer in B-cells inhibitor, alpha	Yes	2,3
1600029D21Rik	placenta-expressed transcript 1 protein precursor	Yes	2,2
Slc26a7	Solute carrier family 26, member 7	Yes	2,2
Slc16a2	Solute carrier family 16 (monocarboxylic acid transporters), member 2	Yes	2,2
Cybrd1	Cytochrome b reductase 1	Yes	2,2
Kcnk1	Potassium channel, subfamily K, member 1	Yes	1,97
Cdk8	Cyclin-dependent kinase 8	Yes	1,9
Vegfa	Vascular endothelial growth factor A	Yes	1,8
Ceacam1	CEA-related cell adhesion molecule 1	Yes	1,8
Emcn	Endomucin	Yes	1,7
Ces3	Carboxylesterase 3	Yes	1,7
Txnip	Thioredoxin interacting protein	Yes	1,7
Timp3	Tissue inhibitor of metalloproteinase 3	Yes	1,7
Rbpms	RNA binding protein gene with multiple splicing	Yes	1,7
Bmp5	Bone morphogenetic protein 5	1	1,5
Slc4a5	Solute carrier family 4, sodium bicarbonate cotransporter, member 5	Yes	1,5

B2m Beta-2 microglobulin Yes 1,5

Genes which decreased in expression at least 1,5-fold with p-values ≤ 0.05 are reported.

*according to EST database (<http://www.ncbi.nlm.nih.gov/nucest>)

¹ Burniat A et al., 2008, according to UniGene (<http://www.ncbi.nlm.nih.gov/unigene>)

² Su AI et al., 2002, according to UniGene (<http://www.ncbi.nlm.nih.gov/unigene>)

Table 2 Genes up-regulated in Pax8^{Cre/fl} thyroid versus Pax8^{Cre/+} thyroid

Gene name	Description	Expressed in thyroid*	Fold change
Car3	Carbonic anhydrase 3	Yes	5,5
Cox8b	Cytochrome c oxidase, subunit VIIIb	1	4,5
Lcn2	Lipocalin 2	1	2,3
Cox7a1	Microfibrillar associated protein 5	1	2,3
Gpc3	Glypican 3	1	2,2
Fstl1	Follistatin-like 1	Yes	2,2
Lgals1	Lectin, galactose binding, soluble 1	Yes	2,1
Scd1	Stearoyl-Coenzyme A desaturase 1	Yes	2,1
Osr1	Odd-skipped related 1	1	2,1
Dbi	Diazepam binding inhibitor	Yes	2
Lum	Lumican	1	2
Dcn	Decorin	Yes	2
Cycs	Cytochrome c, somatic	Yes	1,96
Peg10	Paternally expressed 10	1,2	1,9
Mfap5	Microfibrillar associated protein 5	1	1,8
Itm2a	Integral membrane protein 2A	Yes	1,8
Penk1	Preproenkephalin	1	1,7
S100a10	S100 calcium binding protein A10 (calpactin)	Yes	1,7
Igf2	Insulin-like growth factor 2	1	1,6
Ctsc	Cathepsin C	1	1,6
Scand1	SCAN domain-containing 1	Yes	1,6
Cox7c	Similar to cytochrome c oxidase, subunit VIIc	1	1,6
Ndufb4	NADH dehydrogenase (ubiquinone) 1 beta subcomplex 4	Yes	1,6
Uqcrb	Ubiquinol-cytochrome c reductase binding protein	Yes	1,6
Cox7b	Cytochrome c oxidase subunit VIIb	Yes	1,6
Gja1	Gap junction protein, alpha 1	Yes	1,6
Dpt	Dermatopontin	1	1,57
Cox7c	Cytochrome c oxidase,	1,2	1,5

Gabrq	subunit VIIc Gamma-aminobutyric acid (GABA-A) receptor, subunit theta	1	1,5
Mustn1	Musculoskeletal, embryonic nuclear protein 1	Yes	1,5
Vim	Vimentin	Yes	1,5
Col1a2	Collagen, type I, alpha 2	Yes	1,5

Genes which increased in expression at least 1,5-fold with p-values ≤ 0.05 are reported.

*according to EST database (<http://www.ncbi.nlm.nih.gov/nucest>)

¹ Burniat A et al., 2008, according to UniGene (<http://www.ncbi.nlm.nih.gov/unigene>)

² Su AI et al., 2002, according to UniGene (<http://www.ncbi.nlm.nih.gov/unigene>)

4.3 Cre-mediated recombination of floxed Pax8 allele: deletion of the floxed Pax8 allele mediated by Tg-Cre^{ER}

In order to inactivate Pax8 only in the adult thyroid, a Tg-Cre^{ER} murine line was used. As described in paragraph 1.4.1, this is a transgenic mouse in which the thyroglobulin promoter drives the expression of a chimeric recombinase (Cre^{ER}), in which Cre is fused to a mutated form of the ligand binding domain of the estrogen receptor. Using this model the recombination between the loxP sites takes place only in thyroid follicular cells after a treatment with tamoxifen.

I first generated a Pax8^{fl/+} on a TgCre^{ER} genetic background (Pax8^{fl/+};TgCre^{ER}): these mice were crossed with an heterozygous mouse for the Pax8 null allele (Mansouri et al. 1998), to generate the Pax8^{ko/fl};TgCre^{ER} mice (Fig. 31).

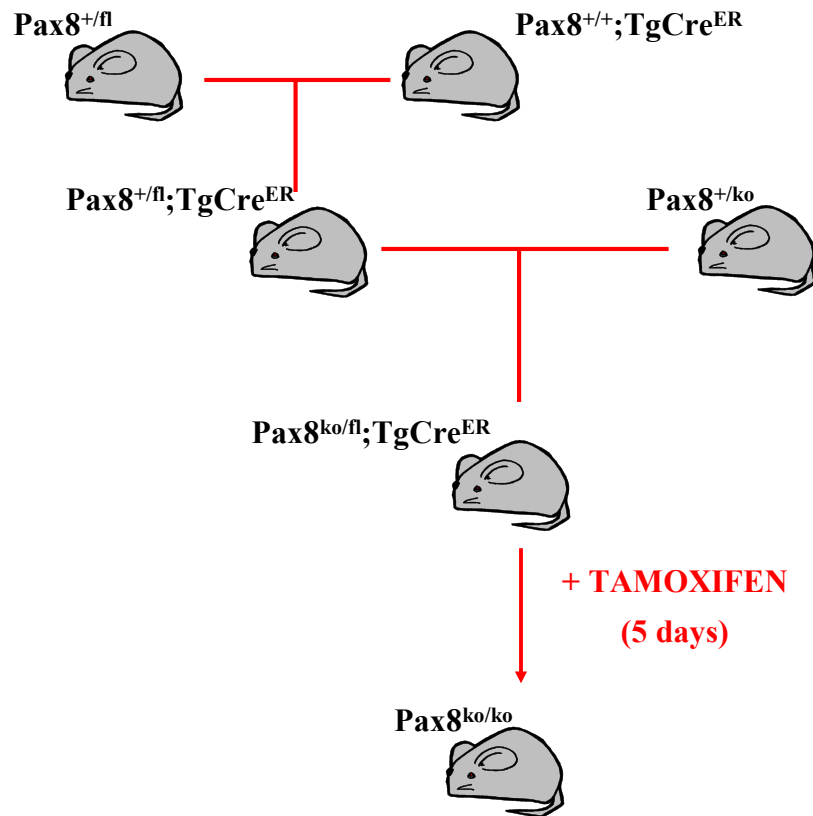


Figure 31 Breeding scheme between the heterozygous mice for the floxed Pax8 allele, the heterozygous mice for the Pax8 knock-out allele and the TgCre^{ER} transgenic mice.

This breeding strategy allowed to obtain a mouse in which a single Cre-mediated recombination event for thyrocyte is sufficient to completely ablate Pax8 in each thyroid cell.

1-month-old mice were subjected to 10 injections of tamoxifen (50mg/Kg body weight) every 12 hours, their thyroids were dissected at 1, 2 and 3 months after the end of the treatment and their morphology was analyzed.

As shown in figure 32, these mice thyroids appeared to be normal with a size and morphology comparable to a wild-type gland. Moreover the histological analysis of these samples revealed that also the follicular structure has not changed.

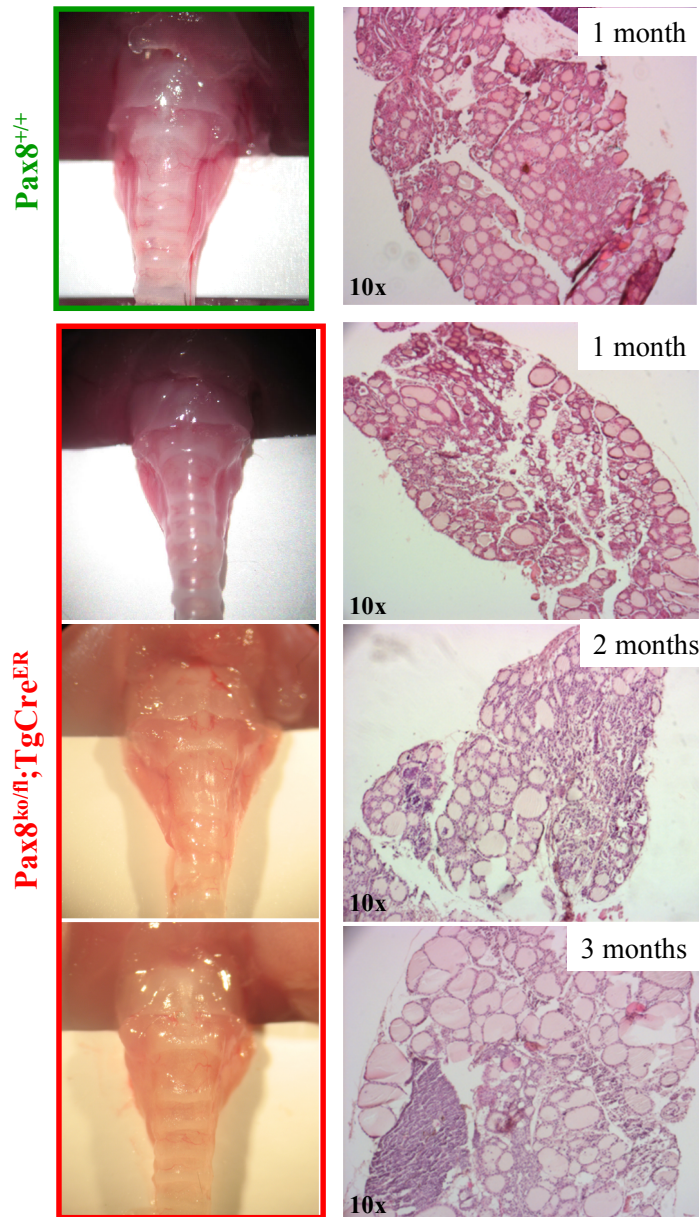


Figure 32 Morphology and histology of Pax8^{ko/fl};TgCre^{ER} thyroids. 1-month-old mice were injected with tamoxifen and their thyroids were dissected after 1, 2 and 3 months from the end of the treatment (b-d and g-h, gross appearance and histological sections respectively). The size of the Pax8^{ko/fl};TgCre^{ER} thyroid is not very dissimilar from a wt thyroid (a,e). (a-d) Morphology of thyroid of mice Pax8^{+/+} and Pax8^{ko/fl};TgCre^{ER}, 1, 2 and 3 months from the end of the treatment, respectively; (e-h) Hematoxylin-eosin staining on paraffin-embedded sections of thyroid of mice Pax8^{+/+} and Pax8^{ko/fl};TgCre^{ER}, 1, 2 and 3 months from the end of the treatment, respectively.

To confirm that the recombination between the two loxP sites correctly happened, a RT-PCR, as described in paragraph 4.2 (Fig. 33), was performed on the thyroids of mice sacrificed 1 month after the end of the treatment.

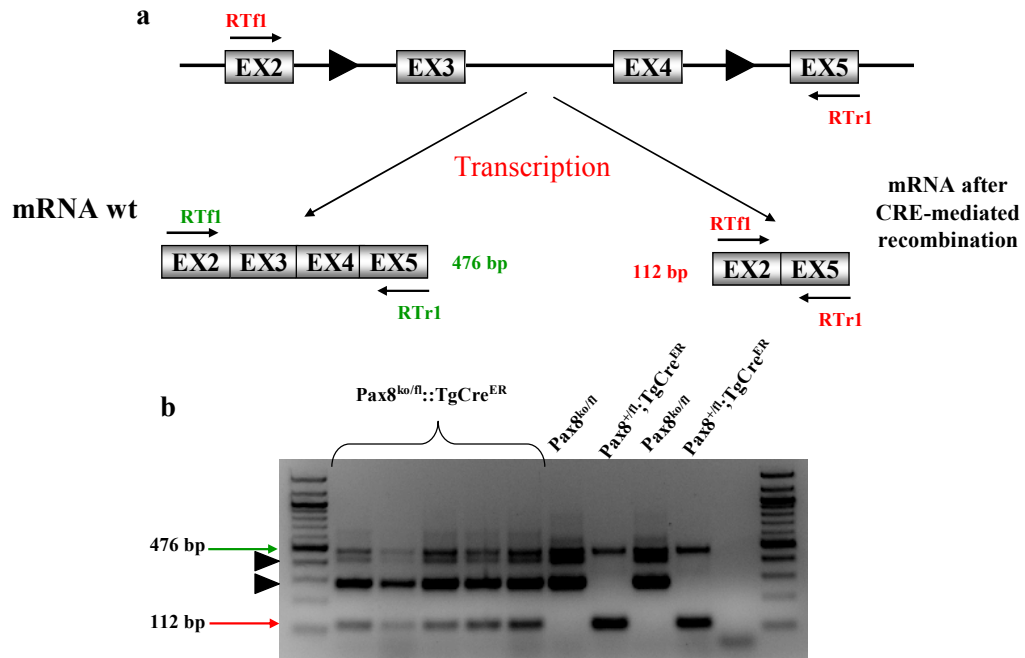


Figure 33 Cre-mediated recombination in $Pax8^{ko/fl};TgCre^{ER}$ mice. (a) The primer RTfl recognizes the exon 2 and the primer RTr1 the exon 5; the expected bands were of 476 bps on the wt transcript and 112 bps on the recombinant one; (b) RT-PCR was carried on five different $Pax8^{ko/fl};TgCre^{ER}$, two $Pax8^{ko/fl}$ and two $Pax8^{+/fl};TgCre^{ER}$ thyroids collected from mice sacrificed 1 month after the end of the treatment. In none of the $Pax8^{ko/fl};TgCre^{ER}$ cDNAs analyzed, the recombination between the loxP sites was complete, in fact, in each sample both the 476 bp wt band and the 112 bp recombinant band are clearly visible.

The coding regions are represented by *grey boxes*, loxP sites by *solid triangles*. *Green and red arrows* indicate wt and recombinant products, respectively. The 300bp and 400bp bands, black arrowheads, are non-specific products in the PCR reaction due to the presence of the Pax8 null allele.

The RT-PCR experiment demonstrated that the Cre-mediated recombination was not complete.

To better evaluate the recombination efficiency, the amount of non-recombinant Pax8-floxed allele was compared with that of the recombinant allele by real-time PCR. For this experiment, $Pax8^{ko/fl};TgCre^{ER}$ 1-month-old mice were treated with tamoxifen, as previously illustrated, and their thyroids were dissected after 1 week and 1 month after the end of the treatment.

To detect all the Pax8 transcripts, I designed a couple of primers on the exons 5 and 6 (F5 and R6 on scheme in figure 33), that amplify a product of 100 bp on both recombinant and non-recombinant transcript. To detect the recombinant product, I designed a primer spanning between the exons 2 and 5, that together with the primer R6 amplify a product of 116 bp on the recombinant template (Fig. 34a).

In figure 34b the expression value of the non-recombinant Pax8 (Pax8 TOT) gene is fixed to 1, while the recombinant gene (Rec Pax8) is expressed as fold of induction on the total Pax8.

In the three samples collected 1 week after the end of the treatment with the drug, the Cre-mediated recombinant transcript is about 50% of the non recombinant one. It is worth noting that instead, 1 month after the end of the treatment the amount of the recombinant product is strongly reduced.

The results obtained from this experiment show that the recombination frequency of this system model is very low and they appear to be in line with the absence of an evident phenotype in Pax8^{ko/fl};TgCre^{ER}.

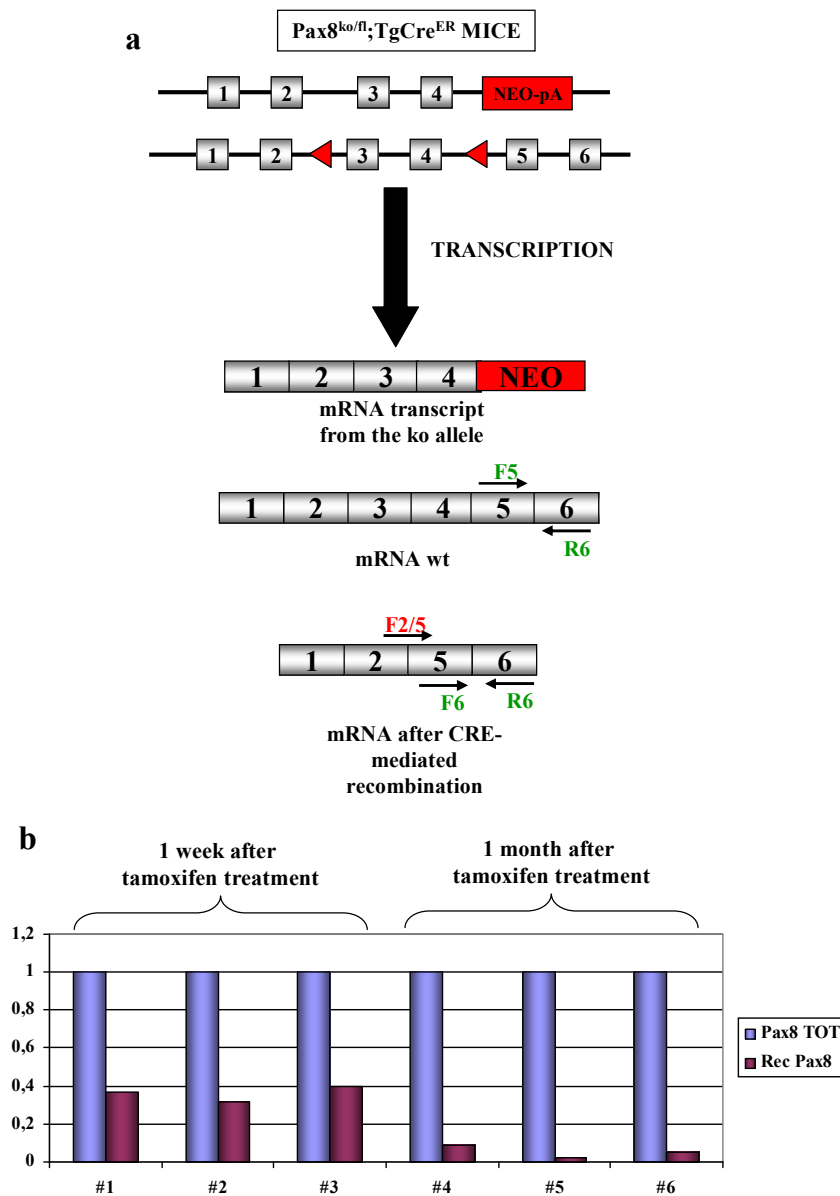


Figure 34 Real-time PCR performed to quantify the recombinant and non-recombinant Pax8 transcript.

Figure 34 Real-time PCR performed to quantify the recombinant and non-recombinant Pax8 transcript. (a) Schematic representation of the Pax8 alleles in Pax8^{ko/fl};TgCre^{ER} mouse. After transcription there are three different Pax8 transcript, one of them derive from the knocked allele and it is interrupted on the exon 4; the other two transcripts are the wt and recombinant mRNAs. The coding regions are represented by *grey boxes*, the neomycin-resistant cassette by a *red box*. The exons are numerated; (b) Real-time PCR performed on RNA extracted from thyroids collected 1 week (#1, 2, 3) and 1 month (#4, 5, 6) from the end of the treatment with tamoxifen. The F5 and R6 are the forward and reverse primer designed on the exons 5 and 6, respectively; the F2/5 primer van amplify only the recombinant transcript.

Pax8 TOT, analysis performed using the couple of primers F5-R6, Rec Pax8, with F2/5-R6.

An inefficient recombination in the Cre/lox system has been frequently described in many cases also in the thyroid (Kusakabe et al. 2006) and in the kidney (Zhang et al. 2009). However, in the murine lines generated, the expression of Cre recombinase is driven by the Tg promoter, that is able to control the expression of thyroglobulin, one of the most expressed genes in the thyroid follicular cell. Furthermore, the use of the transgene TgCre (not inducible) to disrupt a floxed allele of E cadherin (Cali et al. 2007) has already been reported. In this case, Cre-mediated deletion has proven to be efficient.

We therefore considered an alternative hypothesis. In the mouse we generated, Pax8^{ko/fl};TgCre^{ER}, the deletion of the floxed allele completely abolishes the expression of Pax8, since the other allele is already inactivated. Abolishing Pax8 in the adult, as in the embryo, could compromise the survival of the cells. Therefore, in our analysis (Fig. 35) the cells which have undergone recombination might be underestimated, apparently lowering the efficiency of recombination.

We then decided to assess the efficiency of Cre-mediated recombination in Pax8^{+/fl};TgCre^{ER} mice. These mice still have a wild type allele in these mice, so the recombination of the floxed allele should not affect the survival.

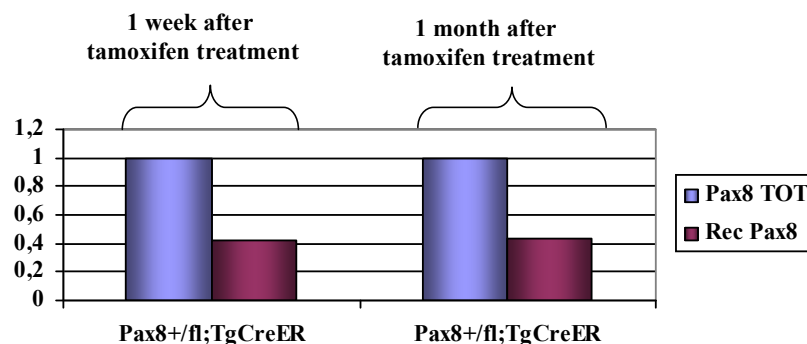


Figure 35 Analysis of the recombination frequency in Pax8^{ko/fl};TgCre^{ER} and Pax8^{+/fl};TgCre^{ER} mice. Real-time PCR performed on RNA extracted from thyroids collected 1 week and 1 month from the end of the treatment with tamoxifen. Pax8 TOT, analysis performed using the couple of primers F5-R6, Rec Pax8, with F2/5-R6. cKO-1W and wt-1W indicate the Pax8^{ko/fl};TgCre^{ER} and Pax8^{+/fl};TgCre^{ER} samples collected 1 week after the end of the treatment. cKO-1M and wt-1M indicate the Pax8^{ko/fl};TgCre^{ER} and Pax8^{+/fl};TgCre^{ER} samples collected 1 month after the end of the treatment.

In this case (Fig. 35), recombination efficiency is almost 100%, in both the samples collected 1 week and 1 month after the end of the treatment. This

result suggests the hypothesis that Cre activation is equally efficient in the Pax8^{ko/fl};TgCre^{ER} mice, but that the cells with Pax8 null phenotype are eliminated. As a consequence, the cells in which recombination has not occurred could proliferate and reconstitute an appropriate organization of the gland.

To confirm this hypothesis, thyroid sections of mice injected with tamoxifen for 5 days and sacrificed 1 week and 1 month after the treatment were stained for Ki-67, to verify the presence of a cellular proliferation activity. In fact, Ki67 is a nuclear protein expressed in all active phases of the cell cycle and for this reason it is used to identify duplicating cells. A higher level of Ki67-expression indicates an increase in mitotic cell activity and proliferation.

The panels in figure 36 show that, a week after the end of the treatment, the number of Ki67 positive cells is comparable between mutant (Pax8^{ko/fl};TgCre^{ER}) and control thyroids (Pax8^{ko/fl}) (Fig. 36 a, b), while in the thyroids collected 1 month after the end of the treatment, the number of these cells increases about 10-fold after Cre recombinase induction (Fig. 36 c, d).

To identify when the proliferation activity exactly starts to be detectable, the immuno-histochemistry assay with anti-Ki67 was also performed on thyroids collected 1 week after the end of the treatment, but in that case no differences in Ki67 expression were detected between the conditional knock out and the controls (Fig. 36 a,b).

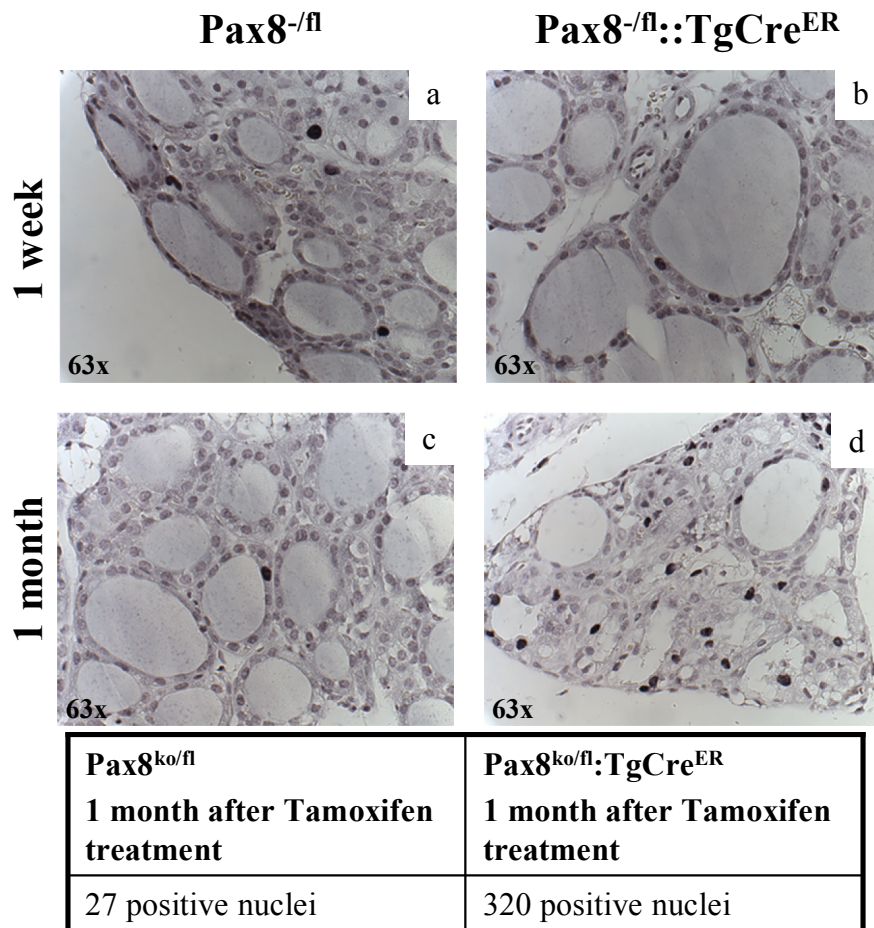


Figure 36 Proliferation assay by immunostaining of Ki67 on paraffin-embedded thyroid sections of Pax8^{ko/fl};TgCre^{ER} and Pax8^{ko/fl} mice. The number of Ki67-positive nuclei in sections of Pax8^{ko/fl};TgCre^{ER} thyroid, dissected 1 week after the end of the treatment with the drug (a,b), is comparable with that found in the control mice. This rate is remarkably increased, almost 10-fold, in the thyroids collected 1 month after the tamoxifen treatment (c,d).

Taken together, these data suggest that the absence of a clear phenotype in the Pax8^{ko/fl};TgCre^{ER} thyroid could be due to the compensatory proliferation of cells in which Pax8 has not been inactivated. Further experiments are required to determine if these cells are completely differentiated cells, or progenitor cells not yet fully differentiated.

CONCLUSIONS

Conventional *Pax8* null mice have been a valuable model to demonstrate that this transcription factor is absolutely required for the development of the thyroid. In this mouse strain the thyroid primordium disappears before thyroid follicular cells accomplish their differentiation (at E11). Hence, *Pax8*^{-/-} mice are not of value for studying the role of Pax8 in the thyroid during the late stages of development and/or in postnatal life. All the available data on Pax8 functions in differentiated cells come from studies on cell lines in culture.

During my thesis work I have generated a novel mice strain that allows a conditional disruption of Pax8 gene in thyroid using the Cre/lox system. This strain has allowed me to study *in vivo* the role of Pax8 in the differentiated thyroid follicular cells.

The phenotype of the *Pax8*^{Cre/fl} mouse is manifest at birth and confirms that Pax8 has a key role in cellular differentiation. Many thyroid-specific genes are down regulated in its absence. Notably, the expression of genes devoted both to hormone production, such as Thyroglobulin TPO, NIS, Na⁺/K⁺-ATPases and to regulative functions, such as Foxe1, Dream, Tshr, is completely abolished. We cannot conclude that all these genes are direct targets of Pax8. As an example, the disruption of Pax8 causes a strong down regulation of Tshr which, together with its cognate ligand TSH, tightly controls the expression of both NIS and TPO as demonstrated in animal models (Postiglione et al. 2002). In any case, Pax8 seems to have a high position in the hierarchy that maintains the differentiation phenotype of thyroid cells. This scenario resembles what occurs during thyroid morphogenesis. At this stage, Pax8 holds a specific upstream role in the genetic regulatory cascade which controls thyroid development (Parlato et al. 2004). According to the hypothesis that Pax8 has a unique role in cellular differentiation, there are the data describing the conditional knock out of *Titf1*, another non-dispensable gene for thyroid development. Mice in which *Titf1* has been disrupted late during organogenesis show both a hypoplastic thyroid and impaired follicular structure but thyroid function is maintained almost normally, with a trend of slight hypothyroidism.

Histological analysis of *Pax8*^{Cre/fl} mice shows that thyroid is hypoplastic and molecular studies reveal a significant up regulation of genes involved in cell death process. An essential role of Pax8 for the survival of thyroid cells is not unexpected, because in conventional *Pax8* null mice the thyroid cell precursors disappear at E11. However, in this strain, the lack of Pax8 is accompanied by loss of both *Titf1* and *Hhex*, making it hard to understand the “prime mover” of cell death phenotype. On the contrary, in *Pax8*^{Cre/fl} mice both *Titf1* and *Hhex* do not appear to be down regulated. Hence, Pax8 absence could be the only factor or at least the major one, responsible for the cell death process. It is worth nothing that the role of Pax8 in cell survival seems to be conserved throughout evolution. In fact, in the nematode *C. elegans*, two *Pax2/5/8*-related

genes play a role in apoptotic mechanisms modulating the transcription of *ced-9*, the *C. elegans* pro-survival *bcl-2* gene (Park et al. 2006).

REFERENCES

- Bedford FK, Ashworth A, Enver T, Wiedeann LM. HEX: a novel homeobox gene expressed during hematopoiesis and conserved between mouse and human. *Nucl. Acid. Res.* 1993; 21,1245-1249 .
- Bogue CW, Ganea GR, Sturm E, Ianucci R, Jacobs HC. Hex expression suggests a role in the development and function of organs derived from foregut endoderm. *Dev Dyn* 2000; 219: 84-89.
- Borutaite V, Brown GC. Mitochondrial regulation of caspase activation by cytochrome oxidase and tetramethylphenylenediamine via cytosolic cytochrome c redox state. *J Biol Chem.* 2007; 282(43):31124-30.
- Bouchard M, Souabni A, Mandler M, Neubuser A, Busslinger M.. Nephric lineage specification by Pax2 and Pax8. *Genes Dev* 2002; 16: 2958-70.
- Bouchard M, Souabni A, Busslinger M. Tissue-Specific Expression of Cre Recombinase from the Pax8 Locus. *Genesis* 2004; 38, 105-109.
- Bradley A. Modifying the mammalian genome by gene targeting. *Curr Opin Biotechnol* 2 1991; 823 – 9 .
- Bradley A. Site-directed mutagenesis in the mouse. *Recent Prog Horm Res* 1993; 48, 237 – 51 .
- Brickman JM, Jones CM, Clements M, Smith JC, Beddington Rs. Hex is a transcriptional repressor that contributes to anterior identity and suppresses Spemann organizer function. *Development* 2000; 127, 2303-2315.
- Buchanan C, Stigliano I, Garay-Malpartida HM, Rodrigues Gomes L, Puricelli L, Sogayar MC, Bal de Kier Joffé E, Peters MG. Glypican-3 reexpression regulates apoptosis in murine adenocarcinoma mammary cells modulating PI3K/Akt and p38MAPK signaling pathways. *Breast Cancer Res Treat.* 2010; 119(3):559-74.
- Burniat A, Jin L, Detours V, Driessens N, Goffard JC, Santoro M, Rothstein J, Dumont JE, Miot F, Corvilain B. Gene expression in RET/PTC3 and E7 transgenic mouse thyroids: RET/PTC3 but not E7 tumors are partial and

- transient models of human papillary thyroid cancers. *Endocrinology* 2008; 149(10):5107-17.
- Cai CL, Liang X, Shi Y, Chu PH, Chu PH, Pfaff SL, Chen J, Evans S. Isl1 identifies a cardiac progenitor population that proliferates prior to differentiation and contributes a majority of cells to the heart. *Dev Cell* 2003; 5(6): 877-89.
- Cali G, Zannini M, Rubini P, Tacchetti C, D'Andrea B, Affuso A, Wintermantel T, Boussadia O, Terracciano D, Silberschmidt D, Amendola E, De Felice M, Schütz G, Kemler R, Di Lauro R, Nitsch L. Conditional inactivation of the E-cadherin gene in thyroid follicular cells affects gland development but does not impair junction formation. *Endocrinology* 2007; 148(6):2737-46.
- Cardoso WV and Lu J. Regulation of early lung morphogenesis: questions, facts and controversies. *Development* 2006; 133: 1611-24.
- Cassuto E, Lash T, Sriprakash KS, Radding CM. Role of exonuclease and protein of phage lambda in genetic recombination. V. Recombination of lambda DNA in vitro. *Proc. Natl. Acad. Sci. USA* 1971;68:1639-43.
- Chadwick BP, Obermayr F, Frischau A. FKHL15, a new human member of the forkhead gene family located on chromosome 9q22. *Genomics* 1997; 41: 390-396.
- Chan QK, Ngan HY, Ip PP, Liu VW, Xue WC, Cheung AN. Tumor suppressor effect of follistatin-like 1 in ovarian and endometrial carcinogenesis: a differential expression and functional analysis. *Carcinogenesis* 2009; 30(1):114-21.
- Chen CY, Kimura H, Landek-Salgado MA, Hagedorn J, Kimura M, Suzuki K, Westra W, Rose NR, Caturegli P. Regenerative potentials of the murine thyroid in experimental autoimmune thyroiditis: role of CD24. *Endocrinology* 2009; 150(1):492-9.
- Civitareale D, Lonigro R, Sinclair AJ, Di Lauro R. A thyroid-specific nuclear protein essential for tissue-specific expression of the thyroglobulin promoter. *EMBO J* 1989; 8, 2537-2542.

- Copeland NG, Jenkins NA, Court DL. Mouse genomic technologies recombineering: a powerful new tool for mouse functional genomics. *Nat. Rev. Genet* 2001; 2:769–79.
- Court DL, Sawitzke JA, Thomason LC. Genetic engineering using homologous recombination. *Annu. Rev. Genet* 2002; 36:361–88.
- Crompton MR, Bartlett TJ, MacGregor AD, Manfioletti G, Buratti E, Giancotti V, Goodwin GH. Identification of a novel vertebrate homeobox gene expressed in haematopoietic cells. *Nucl. Acids. Res.* 1993, 20, 5661-5667.
- D'Andrea B, Di Palma T, Mascia A, Motti ML, Viglietto G, Nitsch L, Zannini. The transcriptional repressor DREAM is involved in thyroid gene expression. *Exp Cell Res* 2005; 305: 166-78.
- D'Andrea B, Iacone R, Di Palma T, Nitsch R, Baratta MG, Nitsch L, Di Lauro R, Zannini M. Functional inactivation of the transcription factor Pax8 through oligomerization chain reaction. *Mol Endocrinol* 2006; 20: 1810-24.
- Damante G, Tell G, Di Lauro R. A unique combination of transcription factors controls differentiation of thyroid cells. *Prog Nucleic Acid Res Mol Biol* 2001; 66: 307-56.
- Dathan N, Parlato R, Rosica A, De Felice M, Di Lauro R. Distribution of the *tif2/foxe1* gene product is consistent with an important role in the development of foregut endoderm, palate, and hair. *Dev Dyn* 2002; 224: 450-6.
- De Felice M, Damante G, Zannini MS, Francis-Lang H, Di Lauro R. Redundant domains contribute to the transcriptional activity of Thyroid Transcription Factor 1(TTF-1). *J Biol Chem* 1995; 270: 26649-26656.
- De Felice M and Di Lauro R. Thyroid development and its disorders: genetics and molecular mechanisms. *Endocr Rev* 2004; 25: 722-46.
- De Felice M, Ovitt C, Biffali E, Rodriguez-Mallon A, Arra C, Anastassiadis K, Macchia PE, Mattei MG, Mariano A, Schöler H, Macchia V, Di Lauro R. A mouse model for hereditary thyroid dysgenesis and cleft palate. *Nat Genet* 1998; 19: 395-398.

- De Felice M, Postiglione MP, Di Lauro R. Minireview: thyrotropin receptor signaling in development and differentiation of the thyroid gland: insights from mouse models and human diseases. *Endocrinology* 2004; 145: 4062-7.
- Di Lauro R and M. De Felice. Factors in differentiation and morphogenesis of the thyroid gland. *Topical Endocrinology* 2003; 21: 13-17.
- Di Palma, T., R. Nitsch, A. Mascia, L. Nitsch, R. Di Lauro, Zannini M. The paired domain-containing factor Pax8 and the homeodomain-containing factor TTF-1 directly interact and synergistically activate transcription. *J Biol Chem* 2003; 278(5): 3395-402.
- Elsalini OA, von Gartzten J, Cramer M, Rohr KB. Zebrafish *hhex*, *nk2.1a*, and *pax2.1* regulate thyroid growth and differentiation downstream of Nodal-dependent transcription factors. *Dev Biol* 2003; 263: 67-80.
- Fabbro D, Pellizzari L, Mercuri F, Tell G, Damante G. Pax-8 protein levels regulate thyroglobulin gene expression. *J Mol Endocrinol* 1998; 21: 347-54.
- Fagman H, Andersson L, Nilsson M. The developing mouse thyroid: embryonic vessel contacts and parenchymal growth pattern during specification, budding, migration, and lobulation. *Dev Dyn*. 2006; 235(2):444-55.
- Fagman H, Grande M, Edsbacke J, Semb H, Nilsson M. Expression of classical cadherins in thyroid development: maintenance of an epithelial phenotype throughout organogenesis. *Endocrinology* 2003; 144: 3618-24.
- Fagman H, Grande M, Gritli-Linde A, Nilsson M. Genetic deletion of sonic hedgehog causes hemiagenesis and ectopic development of the thyroid in mouse. *Am J Pathol* 2004; 164: 1865-72.
- Fagman H, Liao J, Westerlund J, Andersson L, Morrow BE, Nilsson M. The 22q11 deletion syndrome candidate gene *Tbx1* determines thyroid size and positioning. *Hum Mol Genet*. 2007; 16(3):276-85.
- Fontaine J. Multistep migration of calcitonine cell precursors during ontogeny of the mouse pharynx. *Gen Comp Endocrinol* 1979; 37: 81-92.

- Francis-Lang H, Zannini M, De Felice M, Berlingieri MT, Fusco A, Di Lauro R. Multiple mechanisms of interference between transformation and differentiation in thyroid cells. *Mol. Cell. Biol.* 1992; 12, 5793-5800.
- Frigerio G, Burri M, Bopp D, Baumgartner S, Noll M. Structure of the segmentation gene paired and the Drosophila PRD gene set a part of a gene network. *Cell* 1986; 47, 735-746.
- Fukuda, K. and Y. Kikuchi. Endoderm development in vertebrates: fate mapping, induction and regional specification." *Develop. Growth Differ.* 2005; 47: 343-355.
- Ghosh B, Jacobs HC, Wiedemann LM, Brown A, Bedford FK, Nimmakayalu MA, Ward DC, Bogue CW. Genomic structure, cDNA mapping, and chromosomal localization of the mouse homeobox gene, Hex. *Mamm Genome* 1999; 10: 1023-5.
- Goffard JC, Jin L, Mircescu H, Van Hummelen P, Ledent C, Dumont JE, Corvilain B. Gene expression profile in thyroid of transgenic mice overexpressing the adenosine receptor 2a. *Mol Endocrinol.* 2004; 18(1):194-213.
- Grapin-Botton A and Melton M. Endoderm development: from patterning to organogenesis. *Trends Genet* 2000; 16: 124-30.
- Guazzi S, Price M, De Felice M, Damante G, Mattei MG, Di Lauro R. Thyroid nuclear factor 1 (TTF-1) contains a homeodomain and displays a novel DNA binding specificity. *EMBO J* 1990; 9(11): 3631-3639.
- Hamdan H, Liu H, Li C, Jones C, Lee M, deLemos R, Mino P. Structure of the human Nkx2.1 gene. *Biochim Biophys Acta* 1998; 1396, 336-348.
- Hewitt SM, Hamada S, Monarres A, Kottical LV, Saunders GF, McDonnell TJ. Transcriptional activation of the bcl-2 apoptosis suppressor gene by the paired box transcription factor PAX8. *Anticancer Res.* 1997; 17(5A):3211-5.
- Hilfer SR and Brown JW. The development of pharyngeal endocrine organs in mouse and chick embryos. *Scan Electron Microsc* 1984; 4: 2009-22.

- Ho CY, Houart C, Wilson SW, Stainier DY. A role for the extraembryonic yolk syncytial layer in patterning the zebrafish embryo suggested by properties of the hex gene. *Curr. Biol.* 1999; 9, 1131-1134.
- Hoess RH, Ziese M, Sternberg N. P1 site-specific recombination: nucleotide sequence of the recombining sites. *Proc. Natl. Acad. Sci. USA* 1982; 79, 3398-3402
- Hogan B, Beddington R, Costantini F, Lacy E. *Manipulating the mouse embryo: a laboratory manual*, 2nd ed. Cold Spring Harbor, NY: Cold Spring Harbor Laboratory Press 1994.
- Hogan B and Zaret K. Development of the endoderm and its tissue derivatives *Mouse development: Patterning, Morphogenesis, and Organogenesis*. J. Rossant and T. PP. New York, Academic Press 2002; 301-310.
- Horie K, Nishiguchi S, Maeda S, Shimada K. Structures of replacement vectors for efficient gene targeting. *J Biochem* 1994; 115, 477 – 85 .
- Hromas R, Radich J, Collins S. PCR cloning of an orphan homeobox gene (PRH) preferentially expressed in myeloid and liver cells. *Biochem Biophys Res Commun* 1993; 195: 976-983.
- Ikeda K, Clark JC, Shaw-White JR, Stahlman MT, Boutell CJ, Whitsett JA. Gene structure and expression of human thyroid transcription factor-1 in respiratory. *J. Biol. Chem.* 1996; 271, 2249-2254.
- Joiner AL (). *Gene targeting: a practical approach*. Oxford, United Kingdom: IRL Press 1993.
- Kaestner KH, Lee KH, Schlondorff J, Hiemisch H, Monaghan AP, Schutz G. Six members of the mouse forkhead gene family are developmentally regulated. *Proc Natl Acad Sci U S A* 1993; 90: 7628-7631.
- Kaufman MH and Bard J. *The thyroid. The anatomic basis of mouse development*. Kaufman MH and Bard J. San Diego, Academic Press 1999; 165-166.
- Kehrer JP. Lipocalin-2: pro- or anti-apoptotic?. *Cell Biol Toxicol.* 2010; 26(2):83-9.
- Kim G, Lee T, Wetzell P, Geers C, Robinson MA, Myers GT, Owens WJ, Wehr BN, Eckhaus W Michael, Gros G, Wynshaw-Boris A, Levine LR. Carbonic

- Anhydrase III Is Not Required in the Mouse for Normal Growth, Development, and Life Span. *Mol Cell Bio* 2004; 24(22):9942-7
- Kim Y, and Nirenberg M. *Drosophila* NK-homeobox genes. *Proc. Natl. Acad. Sci. USA* 1989; 86, 7716-7720.
- Kimura S, Hara Y, Pineau T, Fernandez-Salguero P, Fox CH, Ward JM, Gonzalez FJ. The T/ebp null mouse: thyroid-specific enhancer-binding protein is essential for the organogenesis of the thyroid, lung, ventral forebrain, and pituitary. *Genes Dev* 1996; 10: 60-69.
- Kimura S, Ward JD, Minoo P. Thyroid -specific enhancer -binding protein/transcription factor 1 is not required for the initial specification of the thyroid and lung primordia. *Biochemie* 1999; 81: 321-328.
- Kozmik Z, Kurzbauer R, Dörfler P, Busslinger M. Alternative splicing of Pax-8 gene transcripts is developmentally regulated and generates isoforms with different transactivation properties. *Mol Cell Biol* 1993;13: 6145-6149.
- Kusakabe T, Kawaguchi A, Hoshi N, Kawaguchi R, Hoshi S Kimura S. Thyroid-specific enhancer-binding protein/NKX2.1 is required for the maintenance of ordered architecture and function of the differentiated thyroid. *Mol Endocrinol.* 2006; 20: 1796-809.
- Lai E, Prezioso VR, Tao WF, Chen WS, Darnell JE Jr. Hepatocyte nuclear factor 3 alpha belongs to a gene family in mammals that is homologous to the *Drosophila* homeotic gene forkhead. *Genes Dev* 1991, 5:416-427.
- Lammert E, Cleaver O, Melton D. Role of endothelial cells in early pancreas and liver development. *Mech Dev* 2003; 120: 35-43.
- Lazzaro D, Price M, De Felice M, Di Lauro R. The transcription factor TTF-1 is expressed at the onset of thyroid and lung morphogenesis and in restricted regions of the foetal brain. *Development* 1991; 113: 1093-1104.
- Le Douarin N, Fontaine J, LeLievre C. New studies on the neural crest origin of the avian ultimobranchial glandular cells. Interspecific combinations and cytochemical characterization of C cells based on the uptake of biogenic amine precursors. *Histochemie* 1974; 38: 297-305.

- Lonigro R, De Felice M, Biffali E, Macchia PE, Damante G, Asteria C and Di Lauro R. Expression of thyroid transcription factor 1 gene can be regulated at the transcriptional and posttranscriptional levels. *Cell Growth Differ* 1996; 7: 251-61.
- Macchia PE, Mattei MG, Lapi P, Fenzi G, Di Lauro R. Cloning, chromosomal localization and identification of polymorphisms in the human thyroid transcription factor 2 gene (TTF2). *Biochimie* 1999; 81: 433-40.
- Mansouri A, Chowdhury K, Gruss P. Follicular cells of the thyroid gland require Pax8 gene function. *Nat Genet* 1998; 19: 87-90.
- Martinez Barbera JP, Clements M, Thomas P, Rodriguez T, Meloy D, Kioussis D, Beddington RS. The homeobox gene Hex is required in definitive endodermal tissues for normal forebrain, liver and thyroid formation. *Development* 2000; 127: 2433-45.
- Meunier D, Aubin J, Jeannotte L. Perturbed thyroid morphology and transient hypothyroidism symptoms in Hoxa5 mutant mice. *Dev Dyn* 2003; 227: 367-78.
- Miccadei S, De Leo R, Zammarchi E, Natali PG, Civitareale D. The synergistic activity of thyroid transcription factor 1 and Pax8 relies on the promoter/enhancer interplay. *Mol. Endocrinol.* 2002; 16, 837-846.
- Minoo P, Su G, Drum H, Bringas P, Kimura S. Defects in tracheoesophageal and lung morphogenesis in Nkx2.1(-/-) mouse embryos. *Devel Biol* 1999; 209: 60-71.
- Motran CC, Molinder KM, Liu SD, Poirier F, Miceli MC. Galectin-1 functions as a Th2 cytokine that selectively induces Th1 apoptosis and promotes Th2 function. *Eur J Immunol.* 2008; 38(11):3015-27.
- Murray D. The thyroid gland. In: Kovacs K, Asa SL, eds. *functional endocrine pathology*. Malden, MA: Blackwell Science, Inc. 1998; 295-380.
- Mythili E, Kumar KA, Muniyappa K. Characterization of the DNA-binding domain of beta protein, a component of phage lambda red-pathway, by UV catalyzed cross-linking. *Gene* 1996;182:81-7.
- Nadeau JH. Modifier genes in mice and humans. *Nat Rev Genet* 2001; 2(3): 165-74.

- Nagy A. Cre recombinase: the universal reagent for genome tailoring. *Genesis* 2000;26:99–109.
- Ohuchi H, Hori Y, Yamasaki M, Harada H, Sekine K, Kato S, Itoh N. FGF10 acts as a major ligand for FGF receptor 2 IIIb in mouse multi-organ development. *Biochem Biophys Res Commun* 2000; 277: 643-9.
- Okladnova O, Poleev A, Fantes J, Lee M, Plachov D, Horst J. The genomic organization of the murine Pax 8 gene and characterization of its basal promoter. *Genomics* 1997; 15: 452-61.
- Ortiz L, Zannini MS, Di Lauro R, Santisteban P. Transcriptional control of the forkhead thyroid transcription factor TTF-2 by thyrotropin, insulin and insulin-like growth factor 1. *J Biol Chem* 1997; 272: 23334-23339.
- Park D, Jia H, Rajakumar V, Chamberlin MH. Pax2/5/8 proteins promote cell survival in *C. elegans*. *Development* 2006; 133, 4193-4202
- Parlato R, Avantaggiato V, De Felice M. TTF-1 and TTF-2 identify two different steps in thyroid morphogenesis. *J. Endocrinol. Invest.* 1999; 22 (Suppl), 4
- Parlato R, Rosica A, Rodriguez-Mallon A, Affuso A, Postiglione MP, Arra C, Mansouri A, Kimura S, Di Lauro R, De Felice M. An integrated regulatory network controlling survival and migration in thyroid organogenesis. *Dev Biol* 2004; 276: 464-475.
- Pasca di Magliano M, Di Lauro R, Zannini MS. Pax8 has a key role in thyroid cell differentiation. *Proc Natl Acad Sci U S A* 2000; 97: 13144-9.
- Pellizzari L, D'Elia A, Rustighi A, Manfioletti G, Tell G, Damante G. Expression and function of the homeodomain-containing protein Hex in thyroid cells. *Nucleic Acids Res* 2000; 28: 2503-11.
- Perrone L, Pasca di Magliano M, Zannini MS, Di Lauro R. The thyroid transcription factor 2 (TTF-2) is a promoter-specific DNA-binding independent transcriptional repressor. *Biochem Biophys Res Commun* 2000; 275: 203-8.
- Plachov D, Chowdhury K, Walther C, Simon D, Guenet JL, Gruss P. Pax8, a murine paired box gene expressed in the developing excretory system and thyroid gland. *Development* 1990; 110: 643-651.

- Poleev A, Wendler F, Fickenscher H, Zannini MS, Yaginuma K, Abbott C, Plachov D. Distinct functional properties of three human paired-box-protein, PAX8, isoforms generated by alternative splicing in thyroid, kidney and Wilms' tumors." *Eur J Biochem* 1995; 228: 899-911.
- Postiglione MP, Parlato R, Rodriguez-Mallon A, Rosica A, Mithbaokar P, Maresca M, Marians RC, Davies TF, Zannini MS, De Felice M, Di Lauro R. Role of the thyroid-stimulating hormone receptor signaling in development and differentiation of the thyroid gland. *Proc Natl Acad Sci U S A* 2002; 99: 15462-7.
- Puppin C, D'Elia AV, Pellizzari L, Russo D, Arturi F, Presta I, Filetti S, Bogue CW, Denson LA, Damante G. Thyroid-specific transcription factors control Hex promoter activity. *Nucleic Acids Res* 2003; 31: 1845-52.
- Romanelli MG, Lorenzi P, Morandi C. Nuclear localization domains in human thyroid transcription factor 2. *Biochim Biophys Acta* 2003; 1643: 55-64.
- Rutledge RG and Cote C (2003). "Mathematics of quantitative kinetic PCR and the application of standard curves." *Nucleic Acids Res.* 31: e93.
- Santisteban P, Acebrón A, Polycarpou-Schwarz M, Di Lauro R. Insulin and insulin-like growth factor I regulate a thyroid-specific nuclear protein that binds to the thyroglobulin promoter. *Mol Endocrinol* 1992; 6:1310-1317.
- Sawitzke JA, Thomason LC, Costantino N, Bubunenko M, Datta S, Court DL. Recombineering: in vivo genetic engineering in *E. coli*, *S. enterica*, and beyond". *Methods Enzymol* 2007; 421:171-99.
- Sequeira M, Al-Khafaji F, Park S, Lewis MD, Wheeler MH, Chatterjee VK, Jasani B, M. Ludgate Production and application of polyclonal antibody to human thyroid transcription factor 2 reveals thyroid transcription factor, 2 protein expression in adult thyroid and hair follicles and prepubertal testis. *Thyroid* 2003; 13: 927-32.
- Shivdasani R. Molecular regulation of vertebrate early endoderm development. *Dev Biol* 2002 249: 191-203.

- Stapleton P, Weith A, Urbanek Z, Kozmik M, Busslinger M. Chromosomal localization of 7 Pax genes and cloning of a novel family member, Pax-9. *Nature Genet.* 1993; 3: 292-298.
- Su AI, Cooke MP, Ching KA, Hakak, Walker JR, Wiltshire T, Orth AP, Vega RG, Sapinoso LM, Moqrich A, Patapoutian A, Hampton GM, Schultz PG, Hogenesch JB. Large-scale analysis of the human and mouse transcriptomes. *Proc Natl Acad Sci U S A.* 2002; 99(7):4465-70.
- Suzuki K, Kobayashi Y, Katoh R, Kohn LD and A. Kawaoi. Identification of thyroid transcription factor-1 in C cells and parathyroid cells. *Endocrinology* 1998; 139: 3014-3017.
- Takuma N, Sheng HZ, Furuta Y, Ward JM, Sharma K, Hogan BL, Pfaff SL, Westphal H, Kimura S, Mahon KA. Formation of Rathke's pouch requires dual induction from the diencephalon. *Development* 1998; 125: 4835-4840.
- Tanaka T, Inazu T, Yamada K, Myint Z, Keng VW, Inoue Y, Taniguchi N, Noguchi T. DNA cloning and expression of rat homeobox gene, Hex, and functional characterization of the protein. *Biochem J* 1999; 339: 111-7.
- Thomas KR and Capecchi MR. Site-directed mutagenesis by gene targeting in mouse embryo-derived stem cells. *Cell* 1987; 51: 503-511
- Thiery JP and J. Sleeman. Complex networks orchestrate epithelial-mesenchymal transitions. *Nat Rev Mol Cell Bio* 2006; 7: 131-42.
- Thomas PQ, Brown A and R. Beddington. Hex: a homeobox gene revealing peri-implantation asymmetry in the mouse embryo and an early transient marker of endothelial cell precursors. *Development* 1998; 125: 85-95.
- Trueba SS, Auge J, Mattei G, Etchevers H, Martinovic J, Czernichow P, Vekemans M, Polak M and Attie-Bitach T. PAX8, TITF1 and FOXE1 gene expression patterns during human development: new insights into human thyroid development and thyroid dysgenesis associated malformations. *J Clin Endocrinol Metab* 2004; 90: 455-62.
- van der Weyden L, Adams DJ, Bradley A. Tools for targeted manipulation of the mouse genome *Physiol Genomics* 2002; 11 , 133 – 64 .

- Zannini M, Francis-Lang H, Plachov D, Di Lauro R. Pax8, a paired domain-containing protein, binds to a sequence overlapping the recognition site of a homeodomain and activates transcription from two thyroid-specific promoters. *Mol. Cell. Biol.* 1992; 12, 4230-4241 ().
- Zannini, M, Avantiaggiato V, Biffali E, Arnone M, Sato K, Pischetola M, Taylor BA, Phillips SJA, Di Lauro R. TTF-2, a new forkhead protein, shows a temporal expression in the developing thyroid which is consistent with a role in controlling the onset of differentiation. *EMBO J* 1997; 16: 3185-3197.
- Zannini MS, Acebron A, De Felice M, Arnone MI, Martin J, Santisteban P Di Lauro R. Mapping and functional role of phosphorylation sites in the Thyroid Transcription Factor 1 (TTF-1). *J Biol Chem* 1996; 271: 2249-2254.
- Zannini MS, Francis-Lang H, Plachov D, Di Lauro R Pax-8, a paired domain-containing protein, binds to a sequence overlapping the recognition site of a homeodomain and activates transcription from two thyroid-specific promoters. *Mol Cell Biol.* 1992; 12: 4230-4241.
- Zhang X, Mernaugh G, Yang DH, Gewin L, Srichai MB, Harris RC, Iturregui JM, Nelson RD, Kohan DE, Abrahamson D, Fässler R, Yurchenco P, Pozzi A, Zent R; beta1 integrin is necessary for ureteric bud branching morphogenesis and maintenance of collecting duct structural integrity. *Development* 2009; 136(19):3357-66.
- Zhang Y, Buchholz F, Muyrers JP, Stewart AF. A new logic for DNA engineering using recombination in *Escherichia coli*. *Nat. Genet.* 1998; 20:123–8.
- Zheng B, Sage M, Sheppard EA, Jurecic V, Bradley A. Engineering mouse chromosomes with Cre-loxP: range, efficiency, and somatic applications. *Mol Cell Biol.* 2000; 20:648–55.